Universitat de Lleida

Corrosion evaluation of molten salts thermal energy storage (TES) systems in concentrated solar power plants (CSP)

Francisco Javier Ruiz Cabañas

Universitat de Lleida

TESI DOCTORAL

Corrosion evaluation of molten salts thermal energy storage (TES) systems in concentrated solar power plants (CSP)

Francisco Javier Ruiz Cabañas

Memòria presentada per optar al grau de Doctor per la Universitat de Lleida
Programa de Doctorat en Enginyeria i tecnologies de la informació

Director/a
Prof. Dr. Luisa F. Cabeza
Prof. Dr. Ana I. Fernández

Tutor/a
Prof. Dr. Luisa F. Cabeza (University of Lleida, Spain)

2020

This page is intentionally left blank.

Departament d'Informàtica i Enginyeria Industrial
Escola Politècnica Superior

Universitat de Lleida

Corrosion evaluation of molten salts thermal energy storage (TES) systems in concentrated solar power plants (CSP)

Memòria presentada per optar al grau de Doctor per la Universitat de Lleida redactada segons els criteris establerts en l'Acord núm. 19/2002 de la Junta de Govern del 26 de febrer de 2002 per la presentació de la tesis doctoral en format d'articles.

Programa de doctorat: Enginyeria i Tecnologies de la Informació
Directors de la Tesis: Dra. Luisa F. Cabeza i Dra. A. Inés Fernández

La Dra. Luisa F. Cabeza, Catedràtica de l'Escola Politècnica Superior de la Universitat de Lleida i la Dra. A. Inés Fernández, Catedràtica del Departament de Ciència de Materials i Química Física de la Universitat de Barcelona.

CERTIFIQUEN:

Que la memòria "Corrosion evaluation of molten salts thermal energy storage (TES) systems in concentrated solar power plants (CSP)" presentada per Francisco Javier Ruiz Cabañas per optar al grau de Doctor s'ha realitzat sota la seva supervisió.

Lleida, juliol 2020

Acknowledgements

I would like to express my sincere thanks to my supervisors Dr. Luisa F. Cabeza and Dr. Ana I. Fernández for her valuable guidance and motivation through the whole PhD.

I would also like to thank the Spanish Government as this work was partially funded by Fondo Tecnológico IDI-20090393 (ConSOLida Cenit 2008-1005), Innterconecta Thesto (ITC-20111050), ENE2011-28269-C03-02, ENE2011-22722, ENE2015-64117-C5-1-R, ENE2015 64117-C5-2-R, RTI2018-093849-B-C31, and RTI2018-093849-B-C32 (with FEDER funds), and RED2018-102431-T. Moreover, the research leading to this Thesis was also funded by European Union's Horizon 2020 research and innovation programme under grant agreement No 657466 (INPATH-TES). Finally, I would like to thank the Catalan Government for the quality accreditation given to the research group of my thesis advisors GREiA (2017 SGR 1537) and DIOPMA (2017 SGR 138). GREiA and DIOPMA are certified agents TECNIO in the category of technology developers from the Government of Catalonia.

I am also grateful to Abengoa for making this Thesis possible. I would like to thank all my colleagues in the Company for the help, support and friendship during all these years, specially to Cristina, Alfonso, Hipólito, Aleix, Edouard, David, María, Carlos, Inma, Jaime, Iván, José Ramón and Joaquín. I would also like to thank Virginia Madina for her continuous support, advice and contribution to this work.

I would like to express my gratitude to my family, specially to my grandparents, my parents and my sister.

Finally, I want to thank Esther and my little Candela their unconditional love.

Resum

El sistema energètic actual, basat en la utilització de recursos d'origen fòssil, provoca impactes mediambientals negatius i desequilibris socioeconòmics que obliguen a definir un nou model de desenvolupament sostenible. La impulsió definitiva de les energies renovables esdevé essencial per assolir els objectius establerts sota les polítiques mundials d'Energia i Clima. La gestionabilitat de la producció és un aspecte clau a l'hora de fer front al canvi del model elèctric actual. El protagonisme creixent de la tecnologia solar termoelèctrica entre el ventall de les energies renovables es centra en la seva capacitat d'adaptar la seva producció a la demanda energètica exigida. La gestionabilitat d'aquest tipus de centrals s'ha aconseguit amb la integració de sistemes d'emmagatzematge tèrmic en les mateixes.

La major part dels sistemes d'emmagatzematge tèrmic, ja sigui els que s'utilitzen a nivell comercial com aquells que es troben en fase de desenvolupament proposen l'ús de sals inorgàniques foses com a medi d'emmagatzematge, fent ús de la seva calor sensible o de la seva calor latent de fusió / solidificació. Aquestes sals presenten una sèrie d'avantatges tals com la seva alta densitat energètica, estabilitat tèrmica, baixa pressió de vapor amb l'afegit d'un cost relativament baix. No obstant, presenten l'inconvenient de la seva alta corrosivitat a altes temperatures el que fa que el disseny i la selecció de materials dels components destinats per a aquest fi es vegin compromesos. Per aquesta raó, la present tesi doctoral es centra en l'anàlisi de l'efecte de la corrosió associat a diversos sistemes d'emmagatzematge en sals per a instal·lacions solars termoelèctriques.

Per un costat, s'han analitzat els fenòmens de corrosió associats a les sals solars (60% $NaNO_3$-40% KNO_3) utilitzades en sistemes d'emmagatzematge tèrmic basat en calor sensible amb sistema de doble tanc per centrals de col·lectors cilindro-parabòlics. Amb aquesta finalitat, s'han realitzat diversos estudis de corrosió in situ a la planta pilot TES-PS10 mitjançant la instal·lació de racks de testimonis de corrosió als tancs de sals. Així s'ha analitzat el comportament del material proposat per a aquests equips envers la corrosió en condicions reals d'operació. A més, al finalitzar l'operació de la instal·lació pilot s'ha dut a terme un estudi post-mortem dels seus components després d'haver estat exposats als nitrats durant més de 30000 hores. Finalment, amb l'objectiu d'abaratir el cost de l'inventari de sals, s'ha analitzat a nivell de laboratori la corrosivitat de diferents mescles de nitrats de baixa puresa.

El segon bloc de la tesi es centra en els sistemes d'emmagatzematge tèrmic en calor latent. Concretament, s'analitza la corrosió associada a la mescla peritèctica 46% LiOH-54% KOH proposta com a material de canvi de fase en un mòdul d'evaporació d'instal·lacions termoelèctriques de generació directa de vapor. D'aquesta forma, s'han dut a terme una sèrie d'assajos a nivell de laboratori amb l'objectiu d'avaluar el comportament envers la corrosió de diferents materials en contacte amb aquests hidròxids. Els resultats obtinguts han permès identificar un aliatge candidat per la construcció de l'intercanviador de calor, el component clau del mòdul d'evaporació proposat en la carcassa del qual s'infiltra la mescla peritèctica.

Resumen

El sistema energético actual, basado en el uso de recursos de origen fósil, provoca impactos medioambientales negativos y desequilibrios socioeconómicos que obligan a definir un nuevo modelo de desarrollo sostenible. La impulsión definitiva de las energías renovables se torna esencial para la consecución de los objetivos establecidos bajo las políticas mundiales de Energía y Clima. La gestionabilidad de la producción es un aspecto clave a la hora de afrontar el cambio del modelo eléctrico. El creciente protagonismo de la tecnología solar termoeléctrica dentro del abanico de energías renovables se centra en su capacidad para adaptar su producción a la demanda energética exigida. La gestionabilidad de este tipo de centrales se ha conseguido mediante la integración de sistemas de almacenamiento térmico en las mismas.

La mayoría de los sistemas de almacenamiento térmico utilizados tanto a nivel comercial como aquellos que están en fase de desarrollo proponen el uso de sales inorgánicas como fluido de almacenamiento ya sea haciendo uso de su calor sensible o calor latente de fusión/solidificación. Las sales presentan una serie de ventajas tales como su alta densidad energética, estabilidad térmica, baja-nula presión de vapor y coste relativamente bajo. No obstante, presentan el hándicap de su corrosividad a alta temperatura lo cual compromete el diseño y la selección de materiales de los componentes de los sistemas de almacenamiento. Por esta razón, la presente tesis doctoral se centra en la evaluación de la corrosividad asociada a distintos sistemas de almacenamiento en sales para instalaciones solares termoeléctricas.

Por un lado, se han analizado los fenómenos de corrosión asociados a las sales solares (60%$NaNO_3$-40%KNO_3) utilizadas en los sistemas de almacenamiento sensible de doble tanque en centrales cilindro parabólico. Para tal fin, se han realizado estudios de corrosión in-situ en la planta piloto TES-PS10 mediante la instalación de racks de corrosión en los tanques de sales. De este modo, se ha analizado el comportamiento a corrosión del material propuesto para dichos equipos en condiciones reales de operación. Además, tras finalizar la operación de la instalación piloto, se ha llevado a cabo un estudio post-mortem de componentes de la instalación tras haber estado expuestos a sales de nitrato durante más de 30000 horas. Finalmente, con el fin último de abaratar el coste del inventario de sales, se ha analizado a nivel de laboratorio la corrosividad de distintas mezclas de nitrato de baja pureza.

El segundo bloque de la tesis se centra en los sistemas de almacenamiento en calor latente. En concreto, se analiza la corrosión asociada a la mezcla peritéctica 46% LiOH-54% KOH propuesta como material de cambio de fase en el módulo de evaporación de instalaciones termoeléctricas de generación directa de vapor. De este modo, se han llevado a cabo ensayos de corrosión a nivel de laboratorio para evaluar el comportamiento a corrosión de distintos materiales en contacto con los hidróxidos. Los resultados obtenidos han permitido identificar una aleación candidata para la construcción del intercambiador de calor, componente clave del módulo de evaporación propuesto, en cuya carcasa se infiltra la mezcla peritéctica.

Summary

The current energy system, based on the use of fossil resources, causes negative environmental impacts and socio-economic imbalances that require a new sustainable development model. The promotion of renewable energies becomes essential for achieving the goals set under global energy and climate policies. The production dispatchability is a key aspect when facing the change of the electrical model. The growing of concentrated solar power (CSP) within the different renewable energies is due to its ability to adapt the production to the required energy demand. The dispatchability of this type of plants has been achieved through the integration of thermal storage systems (TES).

Most TES systems used at commercial scale and in R&D projects propose the use of inorganic salts as storage fluid, using either their sensible heat or latent heat (melting/solidification). Inorganic salts have a number of advantages such as their high energy density, thermal stability, near-zero vapor pressure and relatively low cost. However, they have a handicap associated to their corrosiveness at high temperature, which compromises the materials selection of the components involved in the storage systems. For this reason, the current Thesis focuses on the evaluation of the corrosivity associated to different TES systems integrated in CSP facilities, which use inorganic salts as storage fluid/medium.

On the one hand, it has been analyzed the corrosion phenomena associated with solar salts (60% $NaNO_3$-40% KNO_3) used in sensible heat double-tank storage systems for CSP trough plants. To this end, in-situ corrosion studies have been carried out at the TES-PS10 pilot plant by installing corrosion racks in the salt tanks. In this way, the corrosion behavior of the proposed material for said equipment has been analyzed in real operating conditions. Moreover, after the shut-down of the pilot plant, a postmortem study of different components was performed after being exposed to nitrate salts for more than 30000 hours. Finally, in order to reduce the cost of the salt inventory in TES systems, the corrosivity of different low purity nitrates mixtures has been analyzed at laboratory scale.

The second block of the Thesis focuses on latent heat storage systems. Specifically, it has been analyzed the corrosion associated with the proposed 46% LiOH-54% KOH peritectic mixture as a phase change material in the evaporation module of direct steam generation (DSG) CSP plants. Thus, corrosion tests have been performed at laboratory level to evaluate the corrosion performance of several materials in contact with such hydroxides. Results allowed the identification of a candidate alloy for the construction of a heat exchanger, the key component of the proposed evaporation module within the TES system, in whose shell the peritectic mixture is infiltrated.

Nomenclature

ASTM	American Society for Testing and Materials
CSP	Concentrated Solar Power
CC	Continuous Condition
CTD	Corrosion Testing Device
DSG	Direct Steam Generation
EDS	Energy Dispersive X-ray Spectroscopy
GDP	Gross Domestic Product
HTF	Heat Transfer Fluid
IGA	Intergranular Attack
IGC	Intergranular Corrosion
IC	Intermittent Condition
MAS	Maximum Allowable Stresses
MST	Molten Salts Tower
NACE	National Association of Corrosion Engineers
PTC	Parabolic Trough Collector
PCM	Phase Change Material
PSA	Plataforma Solar de Almería
SEM	Scanning Electron Microscope
SGS	Steam Generator System
SCC	Stress Corrosion Cracking
TES	Thermal Energy Storage
USA	United States of America
UHT	Upper Hot Tank
XRD	X-Ray Diffraction

Contents

List of Figures

List of Tables

1. Introduction

1.1. Concentrated Solar Power. Definition and available technologies

Concentrated solar power (CSP) is the technology, which uses energy coming from solar radiation to generate electricity. This process is carried out in the so-called CSP plants concentrating the direct solar radiation by mirrored surfaces (concentrators) increasing the temperature of a heat transfer fluid (HTF) which circulates through a receiver. Such fluid could execute the thermodynamic conversion cycle in the turbine of the installation producing electricity or could be used as intermediate fluid transferring its energy in a heat exchanger equipment to the final fluid used in the turbine. The different configurations between concentrator and receiver give rise to the main CSP technologies existing today: (i) Parabolic trough collector technology (PTC), (ii) Fresnel technology, (iii) Central Receiver Tower technology and (iv) Parabolic dishes [1].

- Parabolic trough collector technology

The concentrator is a solar tracker parabolic reflector, which concentrates the radiation in a linear receiver located in the focus of the parabola. Then, a parabolic cylinder mirror assembled in a steel structure assuring the alignment to reflect such radiation in the focal line of the parabola where an absorber tube is located constitutes the reflective part. The HTF used for the subsequent generation of electricity circulates inside the absorber tube increasing its temperature [2].

- Fresnel Technology

CSP power plants using Fresnel technology are based, like the others, on heating an HTF to be used in the power block of the plant for electricity production. The peculiarity of this technology regarding the previous one is that reflectors are straight mirror instead of parabolic. These straight mirrors concentrate the solar radiation along a line where the absorber tube is placed through which the HTF circulates. The absorber tube is fixed regarding ground without the possibility of turning together with the mirrors as in the trough technology does [3].

- Central Receiver Tower technology

Central receiver tower technology concentrates the solar radiation using huge mirrors called heliostats. Said mirrors, by means of two axes tracking system concentrate the radiation in the upper part of a tower where the receiver is located. The HTF circulates inside the receiver, which is heated and subsequently is used, directly or indirectly, to generate electricity [4].

- Parabolic dishes

Within this technology the concentrator is constituted by a reflector in the shape of a paraboloid of revolution that concentrates the solar radiation in the focus by following the sun with a two-axis tracker system. In this focus is located a heat engine which transforms the solar radiation in thermal energy and then generates electricity by a Stirling cycle [5].

Following figure (Figure 1) shows the different CSP technologies previously discussed:

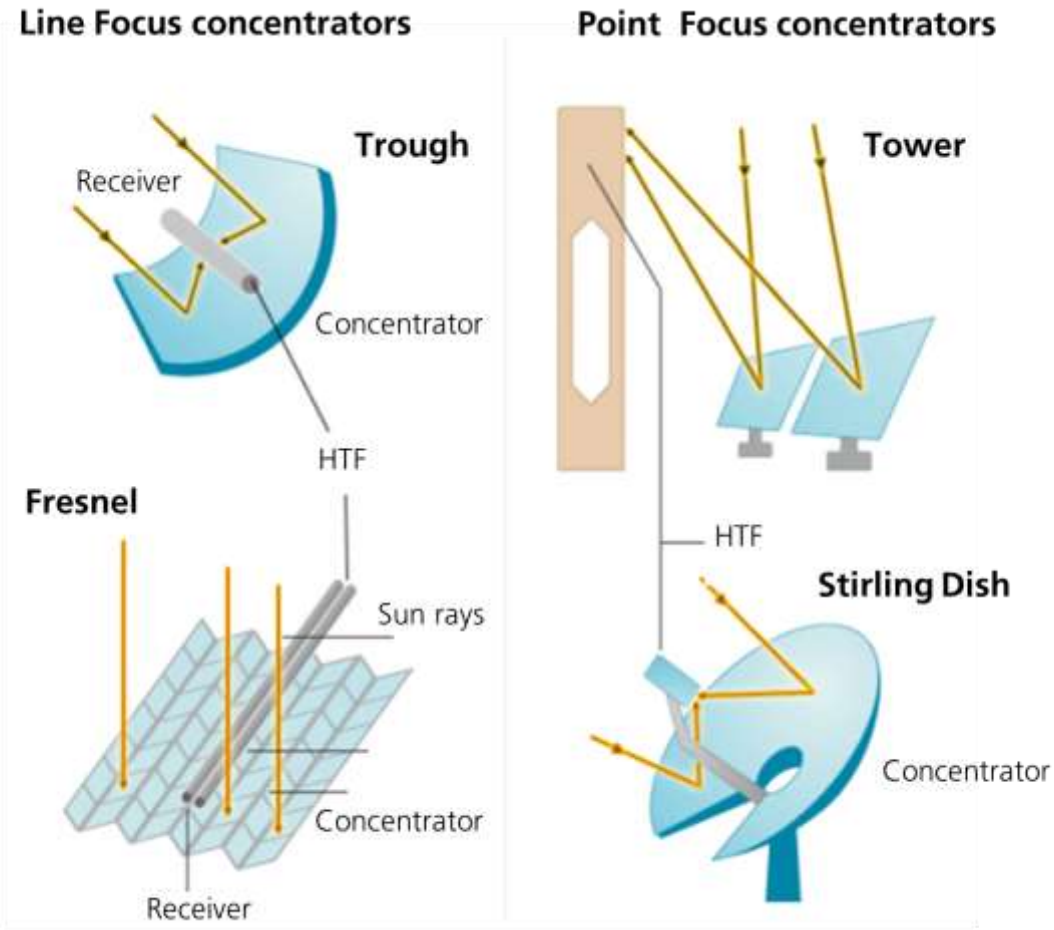

Figure 1. Concentrated Solar Power technologies [6]

1.2. Thermal energy storage systems

The electricity production of a CSP plant must satisfy the daily demand of electricity required by the system. However, it is not feasible to cover all demand periods during the year due to the intermittence of the solar resource. In order to deal with these fluctuations, the electricity production of a CSP installation can be optimized by integrating a thermal storage system. CSP plants become dispatchable when integrating

thermal energy storage (TES) systems, which allow electricity production regardless of the available solar resource. Accordingly, TES system stabilizes the production of electricity expanding the operation of the facility obtaining a better efficiency in the conversion solar to electric. The choice of the proper storage system always depends on the conditions of electricity demand, the specific technology used for the facility among other factors such as the location of the plant.

1.2.1. Classification

Energy storage could be defined in a general way as the accumulation of some form of energy so that it can be used later to carry out an operation. The device in which the energy is stored is called accumulator. Figure 2 shows a classification of energy storage systems.

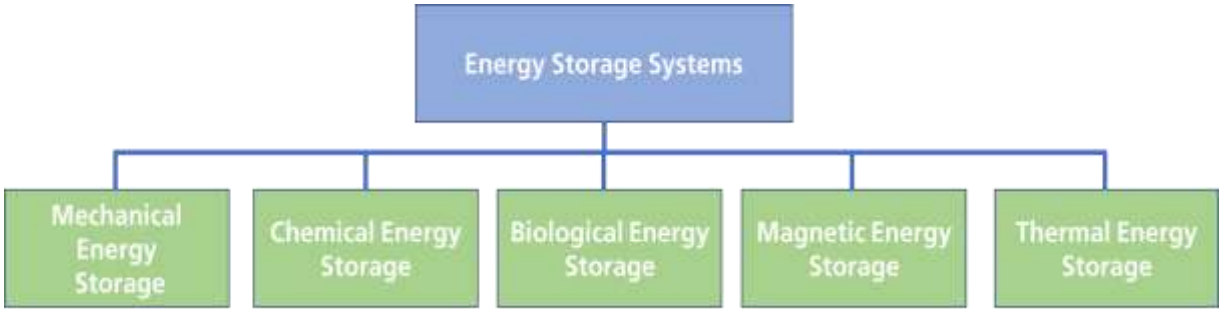

Figure 2. Energy storage systems classification [7]

Taking into account the types of storage systems discussed in Figure 2, the thermal storage is the best candidate to be integrated in CSP plants. Focusing on thermal energy storage, three different types of storage systems could be highlighted: (i) Sensible heat storage systems, (ii) latent heat storage systems and (iii) Storage systems based on chemical reactions.

1.2.2. Thermal storage based on sensible heat

Released or absorbed energy by a material when its temperature is reduced or increased is called sensible heat. Accordingly, the thermal energy can be stored through the change of temperature experienced by a substance. Then, the thermal energy stored by a material could be expressed by the following equation:

$$Q = \rho \cdot C_p \cdot V \cdot \Delta T \quad (1)$$

Where Q is the amount of heat stored, ρ is the density of the substance, C_p is the heat capacity of the material, V is the volume of the storage media and ΔT is the temperature

step associated to the process. Two main phases are typically used in sensible heat storage systems, solid and liquid. Concrete and ceramic materials are proposed in the state of the art for solid storage media due to characteristics such as low cost, good mechanical performance and thermal properties [8]. On the other hand, many liquid storage media have been analyzed in the last years for liquid sensible heat storage systems [9]. Fluids like molten metals, ionic liquids, mineral oils and molten salts were proposed for different applications such as nuclear, petrochemical, solar, among others. Nowadays, the most widely used fluid in the solar industry for liquid sensible storage are molten nitrates as these inorganic salts are selected for the design of TES systems in CSP plants [10-14].

1.2.3. Thermal storage based on latent heat

Thermal energy could be also stored as the latent heat of phase change experienced by a substance. TES systems based on latent heat are considered an efficient alternative regarding others using sensible heat due to higher storage density. There are three main phase changes that could be used for latent energy storage: liquid-gas, solid-solid and solid-liquid being this last one the preferred option for designing latent heat TES systems. Substances used in these applications are typically called phase change materials (PCM). The development of storage systems using PCM has experienced a great growth in the last years [15]. Charging and discharging processes using this technology could be executed at constant temperature providing an advantage in terms of efficiency. In addition, the high energy density, associated to phase change enthalpy in PCM, allows compact storage devices.

PCM could be classified in two different groups: Inorganic and organic PCM [16]. Some examples of inorganic substances using for this application depending on desirable melting/freezing temperature are nitrates, hydroxides, chlorides, fluorides, carbonates and liquid metals. On the other hand, paraffin, fatty acids and sugar alcohols are typical candidates for organic PCM. Both PCM have certain disadvantages that may compromise their application in industrial processes. On the one hand, the low conductivity of these materials leads to deficient efficiencies in the heat transference with the working fluid [17]. On the other hand, the control of thermal expansion during the melting/solidification cycles and solid deposits over heat transfer areas are others important challenges to face about [18, 19].

1.2.4. Thermal storage based on chemical reactions

Thermal energy involved in chemical reactions could be used in TES systems as long as these reactions were reversible. Accordingly, a heat source would excite an endothermic chemical reaction having the possibility of recovering the thermal energy when this energy was necessary in the process. The main advantage associated with this thermal storage mechanism is the high energy density inherent to these systems, which makes

this storage technology very attractive in the future for many applications including solar [20-22]. Some chemical reactions proposed in the state of the art are as follow:

$$NH_3 + \Delta H \leftrightarrow \frac{1}{2} N_2 + \frac{3}{2} H_2 \quad (2)$$

$$CH_4 + H_2O \leftrightarrow CO + 3H_2 \quad (3)$$

$$Ca(OH)_2 \leftrightarrow CaO + H_2O \quad (4)$$

$$CaCO_3 \leftrightarrow CaO + CO_2 \quad (5)$$

$$MgO + H_2O \leftrightarrow Mg(OH)_2 \quad (6)$$

1.2.5. Thermal storage configurations

Once the three main types of thermal storage have been defined, a classification based on the storage concept is carried out within this section being focused on CSP facilities. The different TES systems configurations applicable to CSP plants are presented in the following Figure (Figure 3) [23].

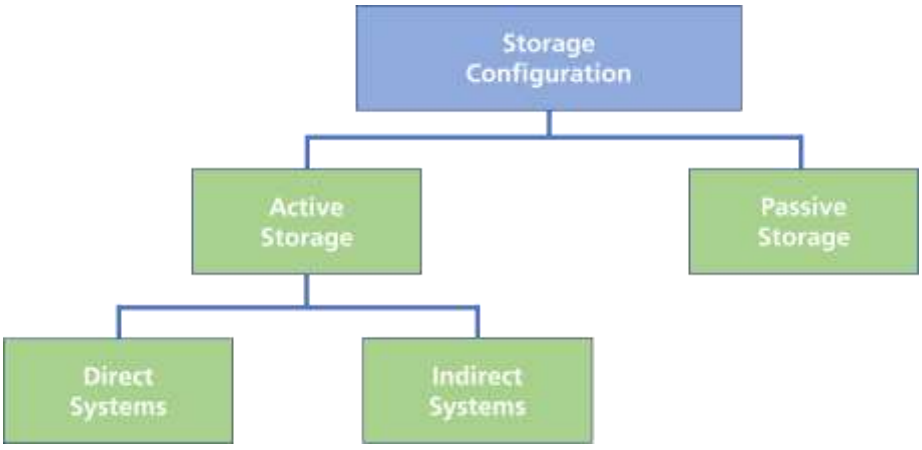

Figure 3. Classification regarding storage concept for CSP plants

1.2.5.1. Active storage Systems

Forced convention processes characterize these types of systems. In this way, the storage medium that is usually stored in one or two tanks circulates through a heat exchanger to carry out the discharge of the storage system. The active systems can be further subdivided into direct and indirect active systems.

Direct Active storage systems

Direct active systems use the same fluid as HTF and storage media avoiding the need of a second fluid in the system. Accordingly, the design of this plant removes the associated cost of heat exchangers used for the thermal transference between the storage fluid and HTF in case both were different. Molten salts tower (MST) plants are typical examples of CSP facilities integrating direct active storage systems. Cold molten salts are stored in the cold tank at 290 °C being pumped to the solar receiver where are heated up to 565 °C. Then, salts are accumulated in the hot storage tank being again pumped to the steam generator system (SGS) to produce superheated steam. This steam is finally used to move the turbine. This operation could be also executed at night or during transients (cloudy periods) allowing the electricity production without solar resource [24].

Figure 4 shows two different plant designs using molten salts as HTF and storage fluid: PTC facility (Figure 4a) and the above explained central solar receiver tower plant (Figure 4b).

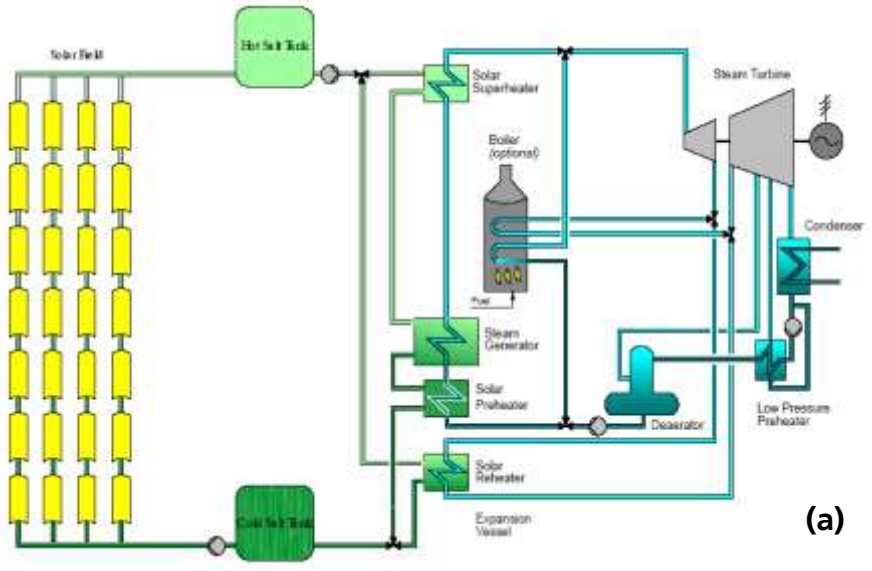

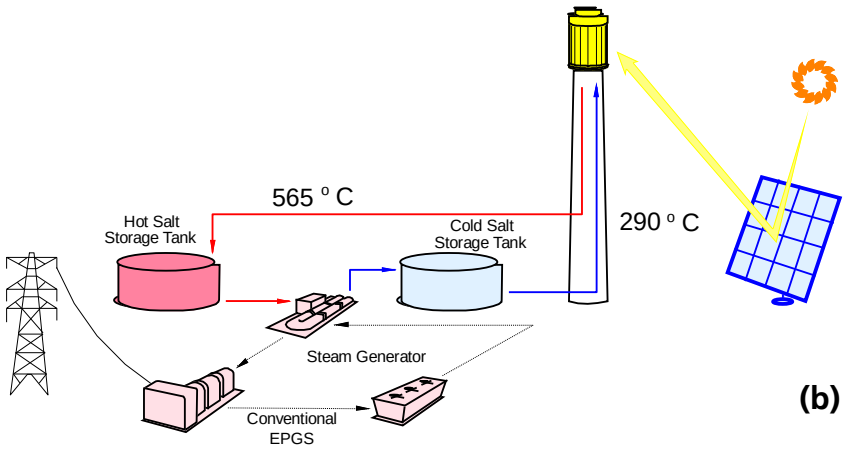

Figure 4. CSP plants with direct active storage systems. a) Molten salts parabolic trough collector facility [25] and b) Molten salts tower facility [26]

Indirect active storage systems

Indirect active storage systems use an HTF circulating through the solar field, which is different to the storage fluid used in the TES system. This power plant arrangement needs an additional heat exchanger regarding facilities designed with direct TES systems to carry out the thermal transference between both fluids [27]. The double tank configuration using molten salts as storage fluid is the most widespread indirect active storage system at commercial scale in CSP plants (Figure 5a). During the charge process of the storage system, cold salts are pumped from the cold tank in which they are stored at 290 °C to a heat exchanger. Part of the synthetic oil heated in the solar field is pumped to this heat exchanger transferring its thermal energy to the salts. Then, salts are stored at 390 °C in the hot tank. During the discharge mode the opposite operation is performed. Then, hot molten salts are used to increase the temperature of the synthetic oil in the above-mentioned heat exchanger. Finally, the synthetic oil is circulated to a SGS to produce superheated steam, which will be used in the turbine to produce electricity. An alternative configuration for indirect active systems is the use of a single tank in the storage system being both fluids stored inside (Figure 5b) [28].

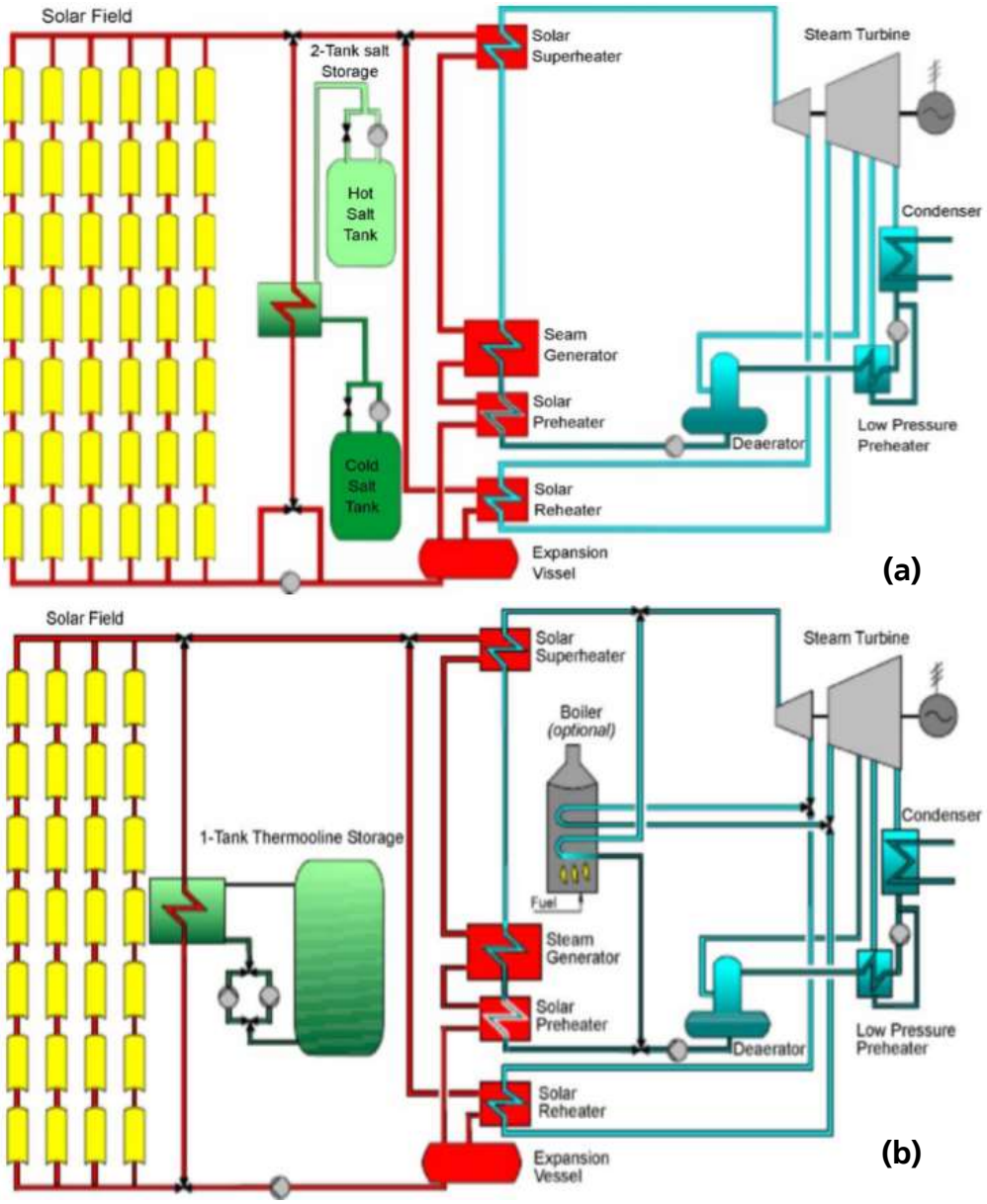

Figure 5. CSP plants with indirect active storage systems [24]. a) PTC facility with double molten salts tank layout, b) PTC facility with single molten salts tank

1.2.5.2. Passive storage systems

The main characteristic of passive storage systems is that the storage medium does not have circulation requiring a HTF, which pass through the storage medium during the charge and discharge cycles of the TES system. Passive systems are usually designed with solid materials such as concrete or ceramics [29-30]. Figure 6 shows a parabolic trough collector facility using a passive storage system with high temperature concrete as storage medium. Another possibility is the use of a PCM in the storage module taking advantage of the high energy density of this type of solutions.

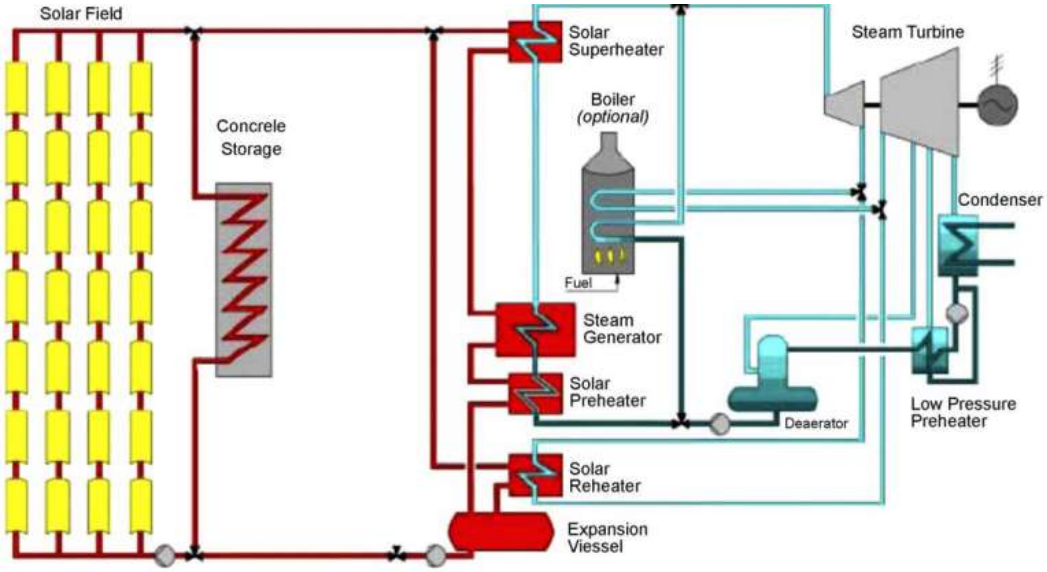

Figure 6. PTC plant using a concrete storage module as TES system [24]

1.3. TES systems in CSP plants

Molten salts are the most widespread fluid in TES systems for CSP plants due to properties such as: (i) high energy density, (ii) low vapor pressure, (iii) high thermal stability and (iv) relative low cost. Important efforts were dedicated in the last years to demonstrate the feasibility of molten salts as storage fluid for large commercial CSP plants by designing and operating facilities at demo scale [31].

Regarding sensible storage systems, four different demo projects could be highlighted. Cesa-1 (Plataforma Solar de Almería (PSA), Spain) and Themis pilot plant (France) were designed using the same inorganic mixture as storage fluid, 53 % $NaNO_3$, 40 % $NaNO_2$ and 7 % $NaNO_3$ by weight [32, 33]. Salts were stored in a double tank storage configuration with temperature rages 200°C-340°C (Cesa-1) and 250°C-450°C (Themis). On the other hand, the Central Receiver Test Facility, CRTF project (United States), evaluated the feasibility of molten salts tower technology using solar salts (60% $NaNO_3$-40%KNO_3 by weight) as HTF [33]. The outlet temperature of the receiver was fixed at 565°C. Finally, TES-PS10 pilot plant was built by Abengoa Solar in Sanlúcar la Mayor (Seville, Spain) to validate the feasibility of integrating a double tank molten salts storage system in a PTC facility. Accordingly, TES-PS10 was connected to Repow PS10 demonstration solar power plant, consisting of a PTC loop (600 m) that uses thermal oil as a HTF and whose thermal output is 2.025 MWth. The storage capacity of TES-PS10 was 8.1 MWhth, four hours at thermal oil loop capacity [34].

These four pilot scale projects showed the technical feasibility of sensible thermal storage with molten salts up to 565 °C being the base for future commercial power plants. Solar Two installation (Barstow, United States) which was able to produce electricity during three hours without solar resource could be considered as the first commercial scale project using molten salts as storage medium [35]. Solar Two had an

inventory of 1350 tons of solar salts stored in two tanks operated in the range 290 °C-565 °C. Nowadays the use of molten salts as sensible storage medium is fully widespread in CSP plants with a high amount of installed MW worldwide. Some interesting examples due to their high storage capacity are Solana Power plant (Arizona, United States) and Cerro Dominador power plant (Chile). Solana provides 280 MW to the grid being designed with six hours of storage [36]. On the other hand, Cerro Dominador which is right now under construction will provide 110MW expanding the electricity production thanks to 17.5 hours storage system allowing the generation during 24 hours [37].

Thermal storage systems based on latent heat have not been commercialized at large scale in CSP plants. Some pilot experiences were developed in the last years mainly focused on direct steam generation (DSG) applications. As an example, a latent TES system prototype (100 kWth) based on $NaNO_3$-KNO_3 mixture and expanded graphite to improve the thermal conductivity was tested at PSA [38]. On the other hand, ITES project evaluated a storage system where PCM latent heat storage was used for evaporation. A prototype with a storage capacity of 1MWh was integrated in a DSG facility. Sodium nitrate was selected as PCM for this project using aluminum fins to increase the thermal conductivity [39].

1.4. Molten salts and corrosion

1.4.1. Introduction

One of the most important challenges in the design of molten salts TES systems is to perform an optimal materials selection for the different equipment and components exposed to the storage medium. In addition to the thermal-mechanical requirements inherent to operation temperature and pressure, the corrosion compatibility with metal alloys is an important boundary condition to take into account in the engineering phase of a CSP plant. In this way, the materials selection and associated corrosion allowances must be optimized fulfilling a twofold purpose: (i) maximize the lifetime of the components matching with the expected operating time of the installation, which is in the range 25-35 years and (ii) minimize costs associated to TES systems increasing competitiveness of CSP facilities.

Corrosion phenomena over metal alloys used in the industry could produce the deterioration of these materials compromising people safety and their validity for the application they were designed for. This problem has associated large economic losses, which could be in the range of 3-4% of gross domestic product (GDP) in industrialized countries [40]. The National Association of Corrosion Engineers (NACE) published an interesting study about costs associated to corrosion issues for the different industrial sectors in the United States of America (USA). Corrosion costs were estimated in 276 billion of dollars, 3.1% of the GDP [41]. These economic losses are in line with studies that estimate that around 10% of worldwide steel production is used to replace corroded material [40]. Apart from the raw material expenses, it must be considered that the energy required for the production of one ton of steel from iron ore would be

enough for the energy supply of an average household for a period of three months [42]. The complete elimination of corrosion cost in the industry is not feasible. However, important investments are dedicated during the different phases of a project, engineering, construction and later operation and maintenance to minimize economical loses associated to corrosion issues [43].

1.4.2. Economic losses associated to corrosion

Economic losses derived from corrosion phenomena could be divided in two different categories: direct and indirect [44]. Direct economic losses are associated to investments performed during the engineering, manufacturing and maintenance stages. Some examples of direct corrosion losses are as follow:

- High cost materials selection to withstand corrosion phenomena during the life of the installation and specification of higher corrosion allowances
- Application of protection technologies such as paints, coatings, inhibitors, among others
- Preventive maintenance tasks to advance any problem associated with excessive corrosion in the system. If the corrosion failure is produced, costs associated to repair/replacement of the affected component

Unlike direct losses, indirect losses due to corrosion are difficult to quantify. Some typical indirect corrosion losses are as follow:

- Non-programmed maintenance shutdowns due to failures produced by corrosion
- Loss of product due to leaks
- Efficiency losses in equipment and components due to the accumulation of corrosion products

1.4.3. Types of corrosion attack morphology

Molten salts corrosion attack over metal alloys could be classified attending to the appearance of the corrosion damage [45-46]. Typical types of corrosion morphologies that could occur in molten salts systems are summarized in the following figure (Figure 7):

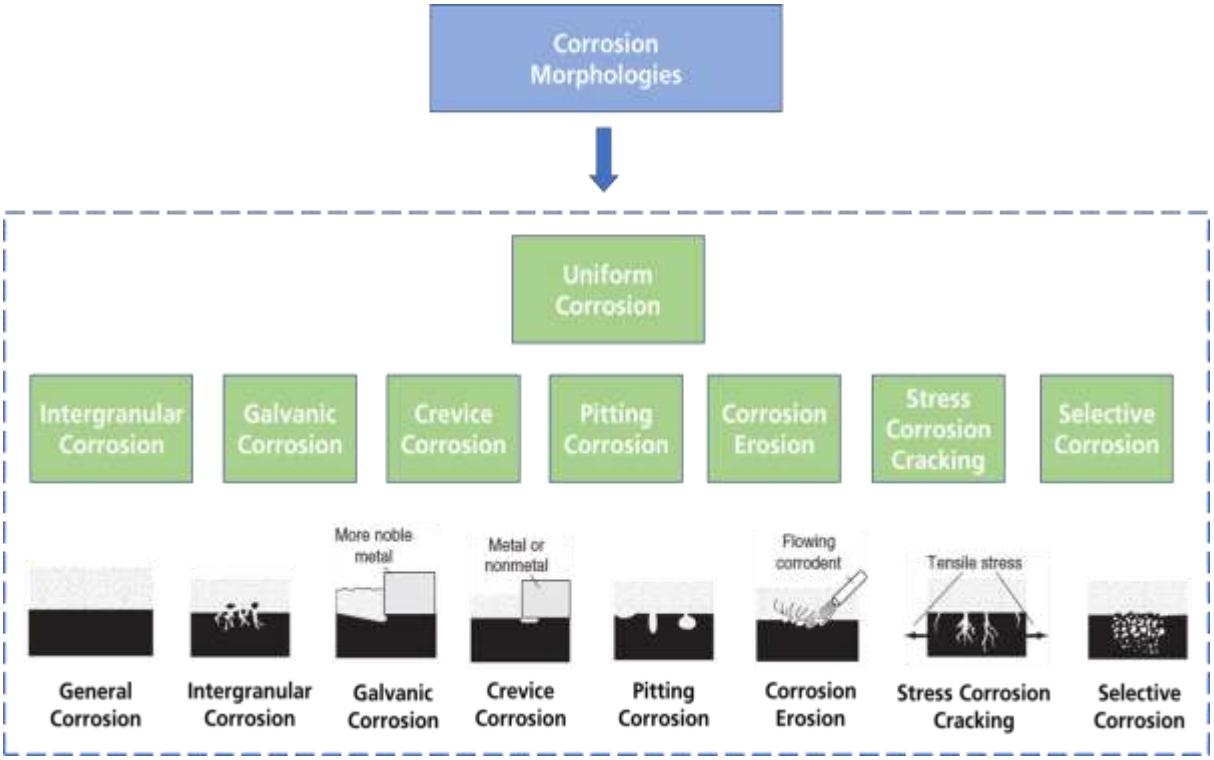

Figure 7. Main corrosion morphologies in molten salts systems

Uniform Corrosion

General or uniform corrosion is characterized by a regular loss of the metal surface exposed to the corrosive medium. Corrosion damage associated to materials affected by general corrosion will be lower or higher depending the passivation created by the corrosion products generated over the base metal. Protection of the corrosion products is strongly dependent of the chemistry of the oxide layer, operation conditions and the aggressiveness of the medium to which the metal is exposed. The quantification of corrosion attack produced by general corrosion could be performed by using the concept of corrosion rate, which is typically expressed as mg/cm^2 or µm/year [47]. Figure 8 shows a typical cross-section micrograph from a carbon steel section affected by general corrosion where a regular oxidation depth is observed.

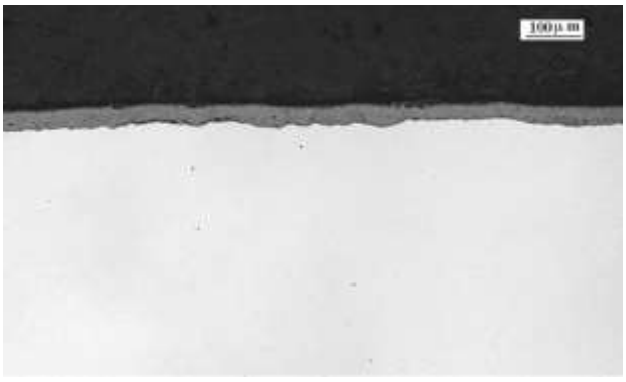

Figure 8. Carbon steel general corrosion [48]

Galvanic corrosion

This type of corrosion is produced when two materials with different electrode potential are electrically connected by exposing to the same electrolyte (Figure 9). Attending to these conditions the less noble material is more affected by corrosion than if it were isolated and the more noble material suffers lower corrosion rate. Galvanic series are powerful tools for the design of installation when dissimilar metals are involved. Within galvanic series, metals are ranked according to their electrode potential in a specific medium, then metals which are very separated in the galvanic series must be avoided [49].

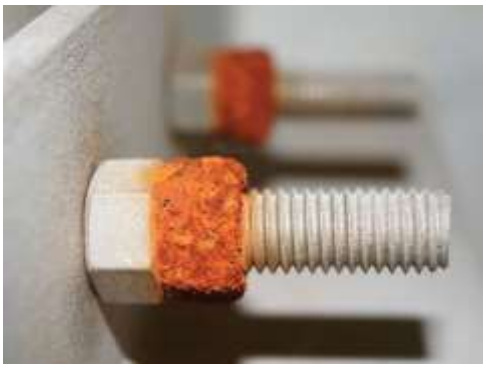

Figure 9. Galvanic corrosion produced in a joint between screw and nut [50]

Crevice corrosion

Crevice corrosion is produced in occluded interstices, beneath deposits and other types of narrow gaps when overlapped areas are created in the design of equipment or components. Accordingly, differential aeration cells are produced promoting the corrosion attack over the metal alloy. There are critical factors affecting to crevice corrosion such as: (i) Aggressiveness of corrosive medium (presence of chlorides, bromides…), (ii) operation conditions such as temperature, (iii) alloy susceptibility to this type of attack and (iv) geometry of the overlapped area [51-53]. Following figure (Figure 10) shows crevice corrosion mechanism and a stainless steel flange affected by crevice corrosion damage after chloride rich medium exposition.

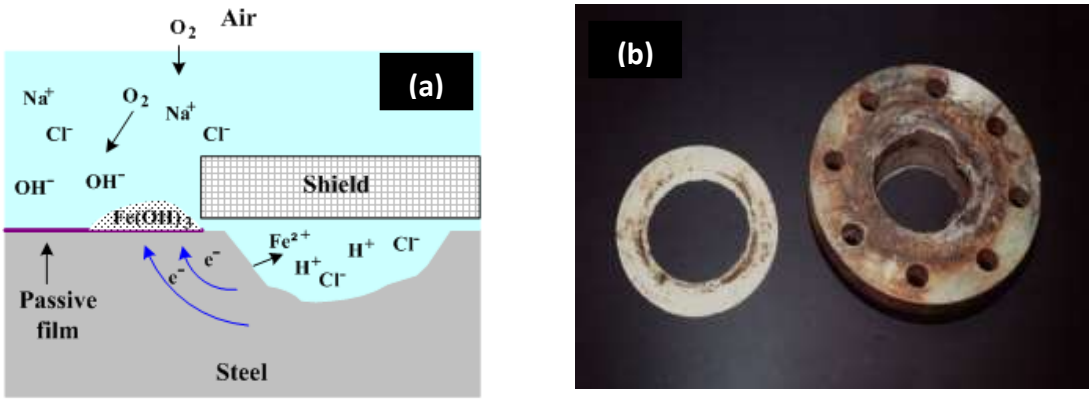

Figure 10. Crevice corrosion. a) Mechanism [54]; b) Flange crevice corrosion [55]

Pitting corrosion

Pitting corrosion, or pitting, is a form of extremely localized corrosion that leads to the creation of small holes in the metal. Pitting corrosion mechanism is similar to crevice one. In this way, the attack over the alloy is produced by the acidification increasing of the medium due to the differential aeration cell created in the affected area. Again, this corrosion damage is accelerated if halides are present in the fluid (Figure 11a). Pits typically require a large incubation period before they could be detected. Moreover, the generation of corrosion products could hide these preliminary pores avoiding the identification during maintenance works leading to catastrophic failures [56].

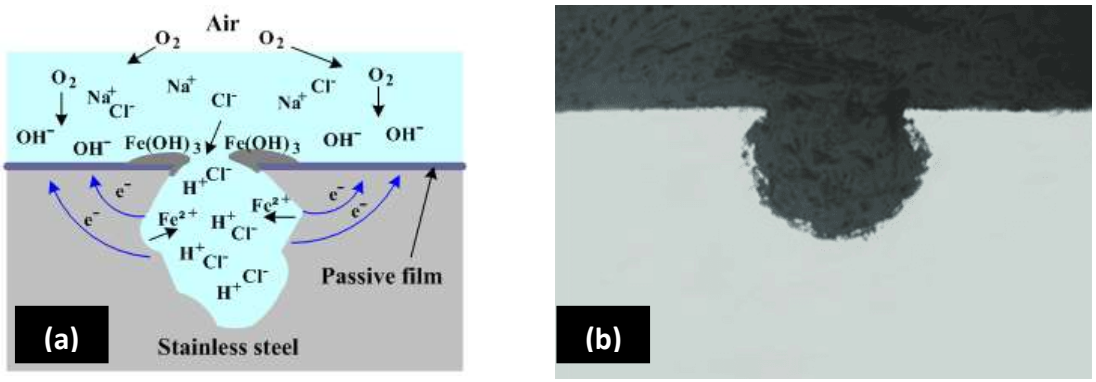

Figure 11. Pitting corrosion. a) Pitting corrosion mechanism [57]; b) Metallographic cross-section showing a pit [58]

Intergranular corrosion

Intergranular corrosion (IGC) is typically produced in the grain boundaries with negligible attack over the grain itself [59]. An electrochemical cell is produced between the grain boundary (anode) and grain (cathode) producing a relative quick corrosion attack over the material. Austenitic stainless steels are prone to intergranular corrosion attack (IGA) (Figure 12). Stainless steel sensitization is produced in the range of 427 °C - 899 °C. At this temperature, Cr depletion is produced by the formation of chromium carbides, which precipitate in the grain boundaries. IGC is highly influenced by the sensitization grade suffered by the alloy and the medium to which the material is exposed [60-62].

Figure 12. Stainless steel part showing IGA [63]

Stress corrosion cracking

This corrosion failure is associated to the combined effect of: i) tensile stresses, ii) exposition to a corrosive medium, iii) material sensitization and iv) adequate temperature and pH. Stress range leading the stress corrosion cracking (SCC) failure is lower than the one needed for a mechanical collapse without the presence of a corrosive atmosphere. Cracking could be intergranular or transgranular depending on the alloy type, medium, among other factors [64]. Figure 13 shows intergranular SCC failure in a heat exchanger tube manufactured in Inconel.

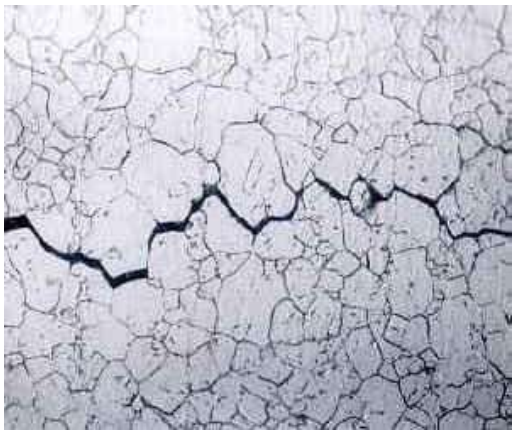

Figure 13. Heat exchanger tube SCC [64]

Selective corrosion

Selective corrosion, also called as dealloying or selective leaching, occurs when there is a preferential corrosion attack over one of the alloying elements of the material. Typical alloys affected by selective leaching are brasses (Figure 14a) and grey casts (Figure 14b). While zinc is removed from brass, iron is detached from grey casts in a corrosion process called graphitization [65-66].

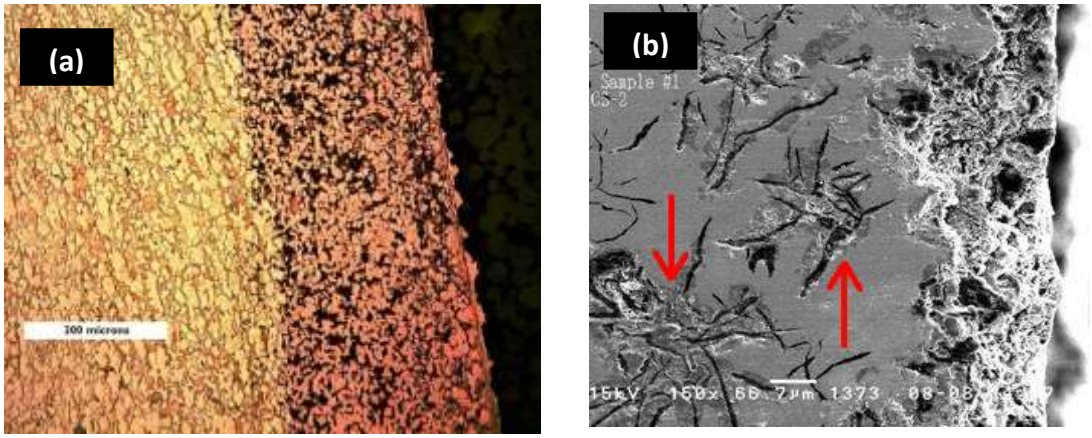

Figure 14. Selective corrosion. a) Brass leaching; b) Grey cast dealloying [67-68]

Corrosion-Erosion

This corrosion damage is characterized by an accelerated attack produced by a corrosive fluid (liquid or gas) which flows through the components of the installation. Mechanical forces remove the oxides layers generated by the alloy avoiding the passivation of the material. Accordingly, new material is continuously exposed to the corrosive medium. Some factors such as fluid velocity, turbulences, solids suspended in the fluid, temperature, among others have an important impact on corrosion-erosion performance [69-70]. Softs materials with low mechanical strength such as copper, aluminum and lead are highly susceptible to corrosion-erosion damage. Figure 15 shows a catastrophic failure in a copper elbow due to corrosion-erosion attack.

Figure 15. Corrosion-Erosion damage over copper pipe [71]

1.4.4. Molten salts corrosion process. Nitrates and hydroxides

All containment materials, which are exposed to molten salts are subjected to molten salts corrosion processes which could be more or less aggressive with the alloy depending on parameters such as alloy composition, fluid nature, fluid impurities, fluid velocity, temperature, among others. In general, corrosion reaction typically proceeds by alloy oxidation generating different types of oxides layers depending on the alloying elements of the materials and process conditions. This stage is followed by metal oxides dissolution in the melt [72]. Molten salts corrosion could also take place by mass transfer phenomena produced in systems with different temperature levels. Then, alloying elements dissolution could be produced in the hot side of the loop being deposited in cold areas.

Following subsections are focused on corrosion processes associated to nitrates and hydroxides salts, which are the fluids evaluated within this Thesis.

1.4.4.1. Nitrates salts corrosion

Nitrates salts corrosion mechanism is inherent to the nitrate-nitrite equilibrium produced at different temperatures, which produces oxide ions. Accordingly, following reversible reduction chemical reaction is produced for molten nitrates [73]:

$$NO_3^- \Leftrightarrow NO_2^- + \frac{1}{2}O_2 \quad (7)$$

Previous reaction leads to the anionic oxidation of the alloy in contact with the nitrates molten salt medium [74]. Then, the following chemical reactions take place. Iron has been chosen as an example of alloying element:

$$Fe + O^{2-} \Leftrightarrow FeO + 2e^- \quad (8)$$

$$3FeO + O^{2-} \Leftrightarrow Fe_3O_4 + 2e^- \quad (9)$$

In addition to oxide ions (O^{2-}), peroxides (O_2^{2-}) and superoxides (O_2^-) ions are typically species formed during the exposition of nitrates bath at high temperatures. These species take an important role in the corrosion of metallic alloys exposed to nitrates salts increasing the aggressiveness of the medium. Chemical reactions associated to the formation of peroxides and superoxides are as follow [75-77]:

$$O^{2-} + NO_3^- \Leftrightarrow NO_2^- + O_2^{2-} \quad (10)$$

$$O_2^{2-} + 2NO_3^- \Leftrightarrow 2NO_2^- + 2O_2^- \quad (11)$$

Corrosion performance of nitrates salts used in CSP applications is highly influenced by impurities. Impurities associated to typical $NaNO_3$ and KNO_3 grades used in solar applications such as chlorides, sulfates, carbonates, and nitrites, among others, could enhance the aggressiveness of nitrates salts over metallic materials. Following table (Table 1) shows typical impurity rages:

Impurities	**$NaNO_3$**	**KNO_3**
Chloride (%wt)	0.10 – 0.60	0.10 – 0.20
Sulfate (%wt)	0.10 – 0.50	0.05 – 0.50
Carbonate (%wt)	0.10	0.02 – 0.10
Nitrite (%wt)	0.02	0.02
Magnesium (%wt)	0.02 – 0.10	0.01 – 0.05

Table 1. $NaNO_3$ and KNO_3 impurity ranges for solar applications [78]

Chlorides have been identified in the state of the art as one of the impurity with higher impact over corrosion. Chlorides increase molten salts aggressiveness over metal alloys due to the formation of chlorine (Cl_2) [79]. Once chlorine has been produced by de combination of chlorides ions, diffusion processes through oxides layer are produced. Chlorine reacts with the steel alloying elements to form metal chlorides at the steel/oxides layer interface. Metal chlorides vapor pressure is relatively high at the interface and the evaporation of these species is produced. Then, metal chlorides diffuse back through the alloy oxides layers cracks and pores produced in the corrosion products of the steel. Finally, metal chlorides are oxidized to metal oxides as magnetite and

hematite. Finally, chlorine is again produced being this specie available to start the process described previously.

$$Fe + Cl_2 \rightarrow FeCl_2(s) \quad (12)$$

$$FeCl_2(s) \rightarrow FeCl_2(g) \quad (13)$$

$$3FeCl_2 + 2O_2 \rightarrow Fe_3O_4 + 3Cl_2 \quad (14)$$

$$2FeCl_2 + \frac{3}{2}O_2 \rightarrow Fe_2O_3 + 2Cl_2 \quad (15)$$

Magnesium is also an important impurity within the solar salts mixture. Magnesium is in the form of magnesium nitrate ($Mg(NO_3)_2$) being an important source of NOx due to the following chemical reaction [80]:

$$Mg(NO_3)_2 \rightarrow MgO(s) + NO_2(g) + NO(g) + O_2(g) \quad (16)$$

Magnesium nitrate thermal degradation is produced in the temperature range 290°C-440°C. Accordingly, the decomposition of this impurity and the formation of NOx gases is within the operation range of PTC and MST CSP facilities. NOx emissions rate is highly influenced by several factors such as molten salts purity, molten salts melting ratio, molten salts temperature, venting process strategy, among others. Depending on the NOx emissions amount, forced venting would be needed to dilute the NOx concentration. Moreover, NOx abatement systems are designed for the treatment of these gaseous streams.

In addition to the environmental issue, the decomposition of the magnesium nitrate could have an important impact over corrosion during the commissioning of the plant [81]. As previously stated, NOx is produced inside TES system due to $Mg(NO_3)_2$ thermal degradation. NOx could react with water coming from tanks preheating process and from salt mixture moisture due to high hygroscopic behavior of nitrate salts. Then, reaction between both substances could produce nitric acid, which condenses in cold zones of the installation:

$$3NO_2 + H_2O \rightarrow 2HNO_3 + NO \quad (17)$$

Nitric acid condensation severely attacks carbon steel producing IGC and SCC in welded and other stresses areas [82].

1.4.4.2. Hydroxides corrosion

The corrosion of metals and alloys produced by molten hydroxides takes place by several processes involving the oxidation of the metal or alloying element in addition to mass

transfer phenomena. Metals or alloys in molten sodium hydroxide are susceptible to mass transfer due to thermal gradients in the melt. This process causes corrosion in the hot areas and the metal removed is deposited in the cool parts of a circulating system. Then, potential tube plugging could be produced in the cold zone of the installation [72, 83]. On the other hand, oxidation by hydroxyl ions is the most typical form of corrosion of metal alloys in hydroxides baths. Attending to the following chemical reaction, hydroxyl ions are reduced to hydrogen and oxide ions. On the other hand, the alloying elements are oxidized to form metal ions. Taking into account a metal designed by "M" with a valence "v" the corrosion process is produced as follows:

$$M + vOH^- \rightarrow M^{v+} + vO^{2-} + \frac{v}{2}H_2 \quad (18)$$

Once metal ions are produced, they could dissolve in the hydroxide melt or may act as oxide-ions acceptors generating an oxide or an oxisalt. In case of oxides are produced, the following chemical reaction shows the general process (Nickel is used as an example of alloying element exposed to molten sodium hydroxide):

$$Ni + 2NaOH \rightarrow NiO + Na_2O + H_2 \quad (19)$$

Two main corrosion morphologies are identified in the stat of the art for alloys exposed to hydroxides melts:

- Pores/cavities formation beneath the surface of the corroded alloys. This phenomenon could be explained by using the corrosion attack over nickel-iron alloys. Iron atoms are oxidized much more quickly than nickel ones. This process produces iron depletion from the surface of the alloy and diffusion of iron from the internal side of the base metal to the outermost surface when iron is again oxidized

- Mixed Corrosion products formation combined with intergranular attack

2. Objectives

The present thesis aims to contribute in providing new knowledge to the thermal energy storage field for CSP applications. The main objective is to study the corrosion performance of two different TES systems identifying a proper materials selection to be used in their design. Then, this thesis will be focused on two TES technologies: (i) Sensible storage systems using solar salts as storage medium in a double tank configuration, which are typically integrated in PTC power plants and (ii) Latent storage systems using molten hydroxides for DSG solar power plants. The first technology is widely used at commercial scale but most of the knowledge about materials compatibility in terms of corrosion is based on laboratory studies. On the other hand, the second TES system is promising to obtain a feasible and economic storage module for DSG plants. However, lack of information is detected in the state of the art about the use of molten hydroxides in this application and associated corrosion performance for metal alloys candidates for this TES system. To fulfil this global objective, several sub-objectives are detailed for each part.

Sensible storage system. Solar salts as storage medium in double tank TES systems:

- To Design an in-situ corrosion-testing device (CTD) to evaluate corrosion phenomena associated to molten salts storage systems
- To analyze corrosion performance of TES-PS10 pilot plant under real operation conditions using corrosion coupons submerged in the storage tanks
- To evaluate metal alloys corrosion performance under low quality molten salts for sensible TES systems
- To carry out corrosion postmortem tests for components extracted from TES-PS10 pilot plant after more than 30000 hours of operation
- To compare results between corrosion performance of coupons submerged in TES-PS10 tanks and postmortem evaluation
- To identify lessons learnt to be used in the design of double tank TES system at commercial scale

Latent storage system. Molten hydroxides as PCM TES system in DSG facilities:

- To evaluate the corrosion performance of four different alloy grades (carbon steel, Cr-Mo alloyed steel, stainless steel and nickel base alloy) exposed to molten hydroxides
- To carry out a technical-economical evaluation of the materials selection of the Steam-PCM heat exchanger used in the TES system proposed for DSG solar power plants

3. PhD thesis structure

The PhD thesis is based on a compendium of five papers; all of them have been already published in SCI journals. The thesis is within the frame of thermal energy storage specifically in the corrosion performance of metal alloys exposed to fluids, solar salts and hydroxides, used as storage media in TES modules. Thesis structure is showed in Figure 16 highlighting two main blocks based on corrosion studies over Sensible TES systems and Latent TES systems.

In the sensible TES system part, **Paper 1** is focused on corrosion studies developed in the TES-PS10 pilot plant to evaluate the expected corrosion performance of tanks alloy under real operation conditions. Therefore, CTD was designed to evaluate corrosion behavior of materials inside high temperature nitrate salts storage tanks in operation. Furthermore, A516 Gr70 carbon steel corrosion coupons (material typically used for the manufacturing of pressure vessels working at temperature below 400 °C) were evaluated at different exposures times by using the CTD in the hot tank of the plant.

On the other hand, **Paper 2** is focused on laboratory tests to analyze the feasibility of using low purity solar salts to reduce the cost of the TES system at commercial scale. The cost of the solar salts is highly influenced by the impurity level required to the mixture. Moreover, chlorides are identified in the state of the art as key impurity to increase the aggressiveness of the salts in terms of corrosion. Then, laboratory tests were launched to identify the corrosion performance of A516 Gr70 in two mixtures with high chlorides content (1.2%wt. and 3%wt.). In addition to corrosion analysis, Ashby approach was used to identify a new materials selection with higher corrosion resistance performance regarding high Cl content solar salts.

Finally, corrosion postmortem tests were carried out over several components extracted from TES-PS10 pilot plant after the shut-down of the facility. **Paper 3** summarizes the main results extracted from the analysis of tank plates (hot and cold tank) and hot pump. Moreover, a detailed analysis was carried out about differences between the corrosion performance of coupons tested in Paper 1 and carbon steel sections analyzed within this Paper 3. Results within this manuscript provide a useful addition to the commercial development of storage systems integrated in PTC plants due to components under evaluation were in operation during more than 30000 hours.

The latent TES system part of the thesis is focused on identifying the proper materials selection for the design of the steam-PCM heat exchanger to be integrated in the TES system of DSG facilities. **Paper 4** evaluates the corrosion performance of three different alloys, A516 Gr70 carbon steel, A316L stainless steel and Inconel 625 nickel base alloy, after being exposed to LiOH-KOH mixture. Accordingly, thermal-corrosive treatments were developed within high temperatures autoclaves at different test times (360°C during 1005 and 2640 hours).

After doing a preliminary materials selection on Paper 4 for the heat exchanger used in the proposed latent TES system, additional efforts were perfomed to optimize the final

design of the equipment. In this way, **Paper 5** proposes the use of chromium-molybdenum alloyed steels as low-cost alternative to stainless steels for tubes and shell manufacturing. Then, corrosion tests were performed using A387 Gr91 coupons exposed to LiOH-KOH mixture at 315°C and 360°C to analyze corrosion rates, oxides layers morphology and chemistry. Additional parameters with high importance over the steam-PCM heat exchanger design such as thermal conductivity, mechanical strength and cost were also discussed.

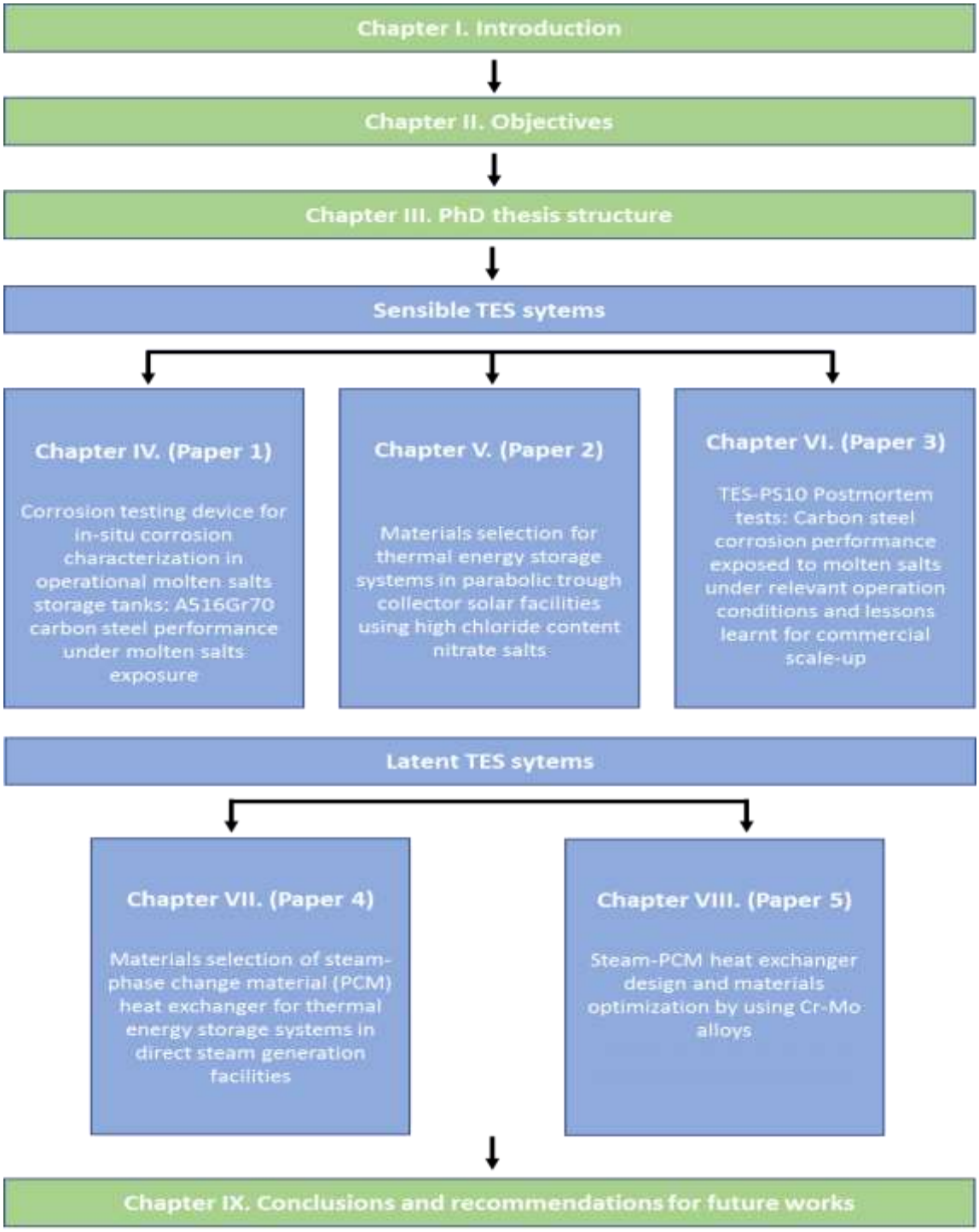

Figure 16. PhD structure scheme

4. Corrosion testing device for in-situ corrosion characterization in operational molten salts storage tanks: A516 Gr70 carbon steel performance under molten salts exposure

4.1. Introduction

The increasing role of CSP technology has been associated to the possibility of integrating large-scale TES systems to adapt electricity production to daily energy demand [1, 24, 84, 85]. Nowadays, the most matured TES systems at commercial scale uses nitrates salts (60% $NaNO_3$ - 40% KNO_3) as storage fluid. One of the most important drawbacks inherent to solar salts is the corrosiveness associated to this fluid at high temperature [23, 86]. Although many authors have evaluated the corrosion performance of metallic alloys in contact with high temperature nitrates salts, lack of information is detected in the state of the art about tests performed at large scale [46, 87-91]. Then, materials selections and design parameters such as corrosion allowances to be used in commercial TES systems are based on laboratory corrosion tests. Lab-scale tests cannot reproduce all the operation and boundary conditions of a commercial storage system. Accordingly, available corrosion performance data should be considered with caution to avoid a wrong materials selection, which jeopardize the lifetime of the TES system under design. In this way, designers use to take security factors such as increase the material grade to be used in the components of the TES system or increase the corrosion allowances to cover uncertainties coming from laboratory results. These security factors increase the cost of the plant reducing the competitiveness of this technology.

The scope of this paper was twofold: i) to design a CTD to check the corrosion performance of metal alloys inside large nitrates salts storage tanks in operation and ii) to fulfill the existing gap on carbon steel corrosion performance data after nitrates salts exposure under relevant operation conditions. Corrosion tests were conducted in the hot tank (390 °C) of the TES-PS10 pilot plant [34, 92] (Figure 17). Nitrogen was used as cover gas in the storage tanks to avoid any explosive atmosphere inside them due to a hypothetic thermal oil leakage in the molten salts-thermal oil heat exchanger.

Figure 17. TES-PS10 pilot plant [34]

A516 Gr70 carbon steel corrosion performance was tested under continuous and intermittent exposure to nitrates salts to compare corrosion aggressiveness between salts atmosphere and salts-N_2 environment. While three different exposure times, 1680 (t1), 4064 (t2), and 8712 hours (t3) were projected for continuous exposition, just one test time (4064 hours) was evaluated for the intermittent one.

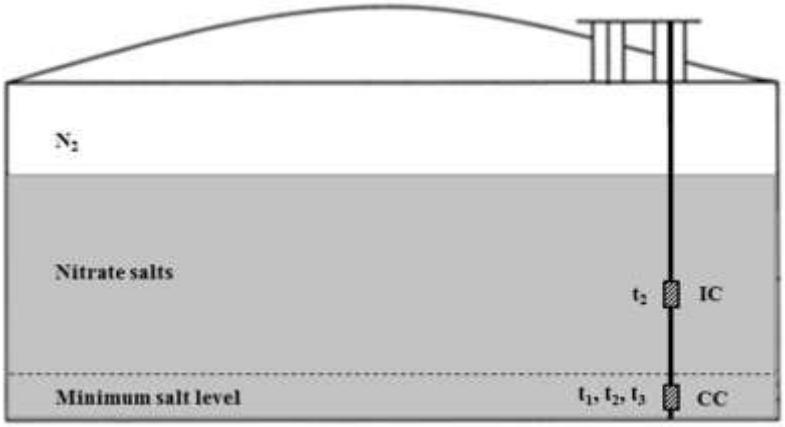

Figure 18. Corrosion tests layout

4.2. Contribution to the state-of-the-art

The first contribution to the state of the art is the design of a feasible and inexpensive tool to evaluate the corrosion performance of metal alloys inside nitrates salts storage tanks in operation. The CTD showed in this study is a safety tool, which was designed adapting the guidelines and recommendations coming from ASTM G4-01 and others ASTM standards about coupons to be used in these types of corrosion tests [93-96]. Main characteristics for a CTD to be used in nitrates storage tanks at a temperature close to 400°C are summarized as follow:

- CTD has a simple design using threaded rods, nuts, washers and rectangular parts to assembly the corrosion coupons to be evaluated

- All the parts used to manufacture the CTD have high corrosion resistant to nitrates salts. The material used for rods, nuts, washers and other parts was Hastelloy C-276

- Galvanic corrosion between coupons and the other metallic parts is avoided by using alumina washers

- The assembly procedure to the storage tanks is also described within the manuscript. A Monel 400 cable is used to suspend the CTD inside the tank. Assembly to the top of the tank is performed by welding a stainless steel connection part to the spare flange. On the other hand, the connection to the bottom was carried out using an Al-Ni-Co magnet to assure that the CTD did not move inside the storage tank

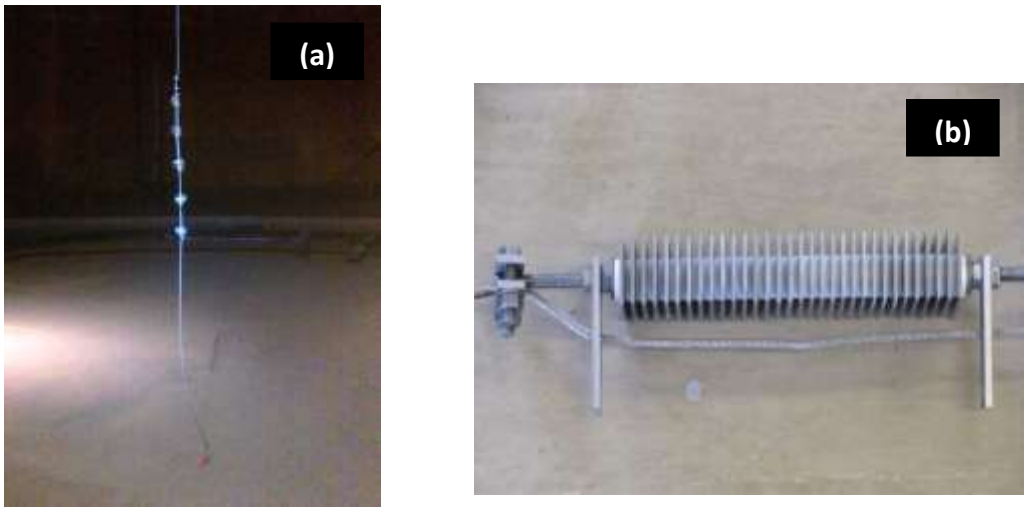

Figure 19. CDT design. a) CTD assembly inside the tank; b) CTD detail

The use of the CTD in operative TES systems for CSP plants has three clear advantages: i) to verify the suitability of the materials selection and associated corrosion allowances specification, ii) powerful tool for preventive maintenance of the system in terms of corrosion and iii) evaluate alternative materials selection in order to obtain a technical-economical optimization for future projects.

This manuscript also contributes to widen up the available information in the state-of-the-art about carbon steel corrosion performance exposed to nitrates salts at 400 °C. Accordingly, this study covers the gap found in this field regarding detailed corrosion data for a typical alloy proposed for the construction of nitrates storage tanks, A516 Gr70, under relevant operation conditions. The main findings after analyzing the corrosion coupons are as follow:

- A516 Gr70 carbon steel showed excellent corrosion performance in contact with nitrate salts at 390 °C for coupons continuously and intermittently exposed to the storage fluid. In addition to low corrosion rates, localized phenomena such as IGC, pitting corrosion, crevice corrosion, among others were not detected

- Coupons exposed continuously to nitrates salts show higher corrosion rates than the ones exposed to N_2/nitrates salts

Test Time (Hours)	Corrosion rate CC (µm/year)	Corrosion rate IC (µm/year)
t1: 1680	22.14	-
t2: 4064	5.46	3.57
t3: 8712	2.14	-

Table 2. Corrosion rates for the different exposures and test times

- A516 Gr70 is passivated developing a thin protective and well adhered oxide layer. Then, corrosion rates decrease through exposition time expecting low corrosion rates for long times

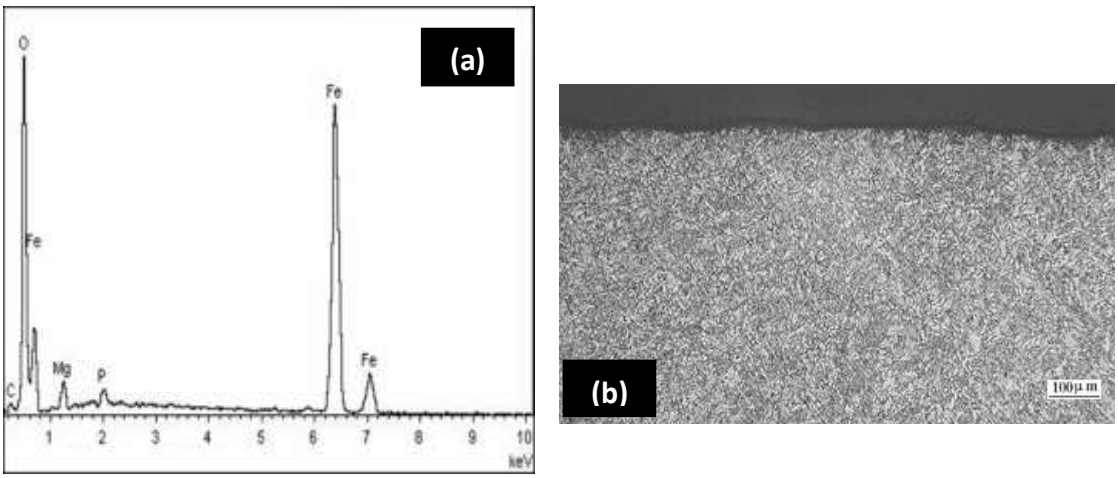

Figure 20. Carbon steel coupon. a) EDS spectrum, b) A516 Gr70 corrosion coupon microstructure after testing

- A516 Gr70 carbon steel is highly recommended for long term service in commercial TES systems due to the low cost of this alloy and negligible corrosion damage produced by the nitrates

4.3. Contribution of the candidate

The candidate carried out the design of the CTD specifying the materials to be used for the assembly of the tool following the guidelines proposed in the ASTM standards. Moreover, the candidate was responsible to define the procedure for CTD installation in the storage tank and for the removal one. The candidate also led the corrosion experimental program defining the type of corrosion coupons to be tested, test times and the characterization to be performed after coupons removal to analyze the corrosion performance of A516 Gr70 alloy. The evaluation and discussion of the results was also in charge of the candidate leading the writing of the manuscript. Finally, the candidate was responsible to summarize all the lessons learned obtained from this study generating a set of specifications to be used in commercial projects such as nitrates salts storage tanks materials selection, nitrates salts storage tanks corrosion allowances and corrosion preventive maintenance in commercial TES system using CTD.

4.4. Journal Paper

Solar Energy Materials & Solar Cells 157 (2016) 383–392

Contents lists available at ScienceDirect

Solar Energy Materials & Solar Cells

journal homepage: www.elsevier.com/locate/solmat

Corrosion testing device for in-situ corrosion characterization in operational molten salts storage tanks: A516 Gr70 carbon steel performance under molten salts exposure

F. Javier Ruiz-Cabañas [a], Cristina Prieto [a,*], Rafael Osuna [a], Virginia Madina [b], A. Inés Fernández [c], Luisa F. Cabeza [d]

[a] Abengoa Research, C/Energía Solar nº 1, Palmas Altas, 41014 Sevilla, Spain
[b] Materials for Energy and Environment Unit, Tecnalia Research and Innovation, Mikeletegi Pasealekua 2, 20009 San Sebastián, Spain
[c] Department of Materials Science & Metallurgical Engineering, Universitat de Barcelona, Martí i Franquès 1-11, 08028 Barcelona, Spain
[d] GREA Innovació Concurrent, Universitat de Lleida, Edifici CREA, Pere de Cabrera s/n, Lleida, Spain

ARTICLE INFO

Article history:
Received 4 April 2016
Received in revised form
16 May 2016
Accepted 1 June 2016

Keywords:
Molten salt corrosion
Corrosion testing device (CTD)
Solar energy
Thermal energy storage (TES)
Sensible heat, solar salts

ABSTRACT

Concentrated solar power (CSP) generation is becoming a very important player within the renewable energy sector thanks to increased introduction of these facilities into the conventional electricity market. CSP plants become dispatchable when integrating thermal energy storage (TES) systems which allow electricity production at any time of the year. Sensible TES using nitrate salts mixtures as storage fluid are the most extended arrangement for commercial CSP facilities. In addition to storage time, dimensions, thermal-mechanical requirements, among others, corrosion compatibility between high temperature nitrate salts, and structural materials is a key factor to take into consideration for the final storage system design. Many scientific contributions have been developed regarding metallic alloys corrosion performance in nitrate salts at laboratory scale. Accordingly, lack of technical background is identified about nitrates corrosion in relevant operation conditions. Therefore, a corrosion testing device (CTD) was designed to evaluate corrosion behavior of structural materials inside high temperature nitrate salts storage tanks in operation. Furthermore, A516 Gr70 carbon steel was evaluated at different exposures times by using the CTD in the TES-PS10 pilot plant. Results reported within this study show the feasibility of the CTD to be used at commercial scale allowing corrosion preventive maintenance practices and materials selection optimization. Moreover, A516 Gr70 carbon steel displayed an excellent corrosion performance after nitrate salts exposure being recommended for long time service under continuous and intermittent exposure to nitrate salts. In addition to low corrosion rates, carbon steel generated protective and well adhered iron oxide layers without significant localized phenomena. Finally, negligible susceptibility to crevice and stress corrosion cracking (SCC) phenomena is showed by carbon steel under test conditions.

Ruiz-Cabañas F.J., Prieto C, Osuna R., Madina V., Fernández A.I., Cabeza L.F. Corrosion testing device for in-situ corrosion characterization in operational molten salts storage tanks: A516 Gr70 carbon steel performance under molten salts exposure. Solar Energy Materials and Solar Cells, 2016; 157: 383-392

https://doi.org/10.1016/j.solmat.2016.06.005

5. Materials selection for thermal energy storage systems in parabolic trough collector solar facilities using high chloride content nitrate salts

5.1. Introduction

One of the most important drawbacks inherent to solar salts is the corrosiveness associated to this fluid at high temperature. Accordingly, nitrates salts used for CSP applications are high quality $NaNO_3$ and KNO_3 grades containing low amount of impurities which increase the final cost of the storage medium. TES system cost breakdown for a 50 MW PTC installation with storage capacity from 1 hour to 15 hours is detailed in Figure 21 [27]. Molten salts cost is in the range of 23% to 48% of the total one depending on installed storage capacity.

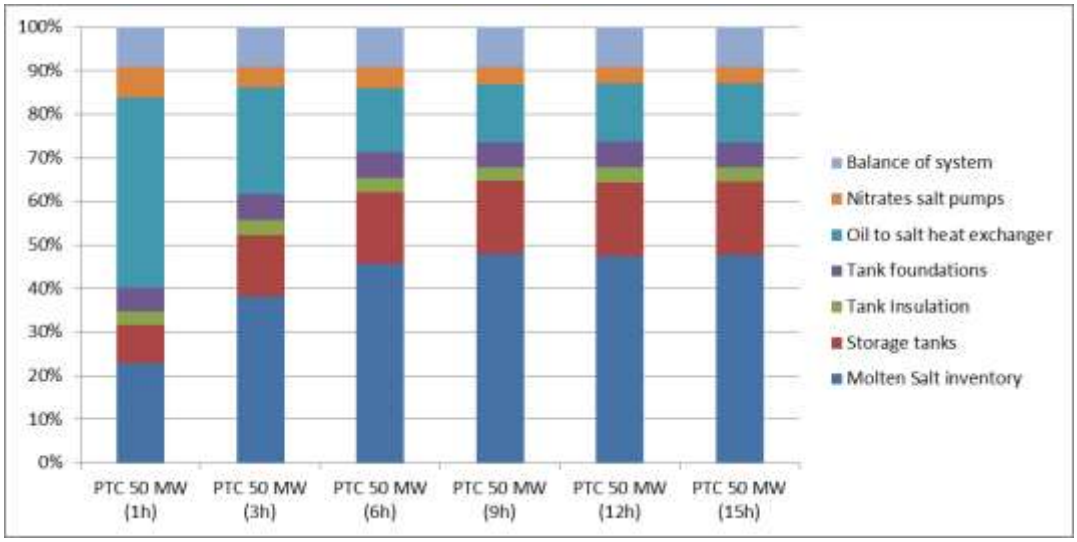

Figure 21. Molten salts TES energy cost breakdown for 50 MW PTC plant with different storage capacities (1, 3, 6, 9, 12 and 15 hours). Adapted from [27]

Costs associated to current nitrates salts used in CSP TES systems are highly influenced by the final purity provided by the supplier. Then, the use of nitrates salts with higher impurity levels would reduce the cost of molten salts inventory and therefore the investment cost of the storage systems. One of the challenges of selecting low quality nitrates salts for high temperature CSP applications is the chloride content increasing (main impurity in industrial grades) which has been identified in the state of the art as one of the impurities with higher impact over corrosion [77, 79, 87, 97].

This paper is focused on the feasibility of using high-chlorides content nitrates salts as storage medium in PTC CSP installations. Then, thermal-corrosive treatments at 400°C were performed to evaluate the compatibility between A516 Gr70 carbon steel and molten salts. Two nitrates mixtures with a total amount of 1.2% Cl^- (Solar_Salt_1.2%Cl) and 3%Cl^- (Solar_Salt_3%Cl) were analyzed in this study. Different corrosion coupons were manufactured to analyze different corrosion damages such as uniform corrosion, SCC, crevice corrosion, among others (Figure 22).

Figure 22. Corrosion coupons assembly to metallic tree inside test crucibles before adding the salt

Laboratory tests within this study face the following purposes: (i) To identify the corrosion mechanism induced by nitrate salts with high chlorides content (1.2% and 3% by weight) over A516 Gr70 carbon steel. (ii) To quantify A516 Gr70 corrosion rates, analyze the performance of welded joints and evaluate SCC and crevice corrosion susceptibility. (iii) To compare results obtained in this study with carbon steel corrosion performance in the TES-PS10 pilot plant (Paper 1 within this Thesis). (iv) To discuss the feasibility of using solar salts with higher impurity levels at commercial scale, with the current materials selection of PTC CSP plants; and, finally (v) To evaluate a higher corrosion resistant materials selection for this application.

5.2. Contribution to the state-of-the-art

Several authors reported interesting results about the influence of chloride content in the corrosion performance of carbon steel showing a dependency between corrosion rates and chlorides percentage. However, these results are associated to short corrosion tests, which would be insufficient for a detailed evaluation of corrosion mechanism or longer thermal-corrosive treatments analyzing the effect of chloride content up to 1% by weight. Then, this study covers the lack of knowledge about long-term corrosion tests with nitrates salts containing chloride percentages higher than 1% by weight, which would analyze the effect of low purity salts over metallic materials used in CSP facilities. Moreover, this manuscript provides information about stress corrosion cracking and crevice corrosion phenomena for A516 Gr70 carbon steel after being exposed to high chloride content nitrate salts for 1581 hours.

A516 Gr70 carbon steel characterization by optical and SEM microscopy showed that corrosion products, mainly composed by hematite and magnetite, developed during both tests (Solar_Salt_1.2%Cl and Solar_Salt_3%Cl) were easily spalled detecting lack of adherence to base metal. Furthermore, oxides layers over metallic coupons tested in the sample with a chloride content of 3% by weight displayed higher porosity and

delamination (Figure 23). A516 Gr70 carbon steel is found to be resistant to SCC and crevice corrosion for mixtures containing up to 3% by weight of chlorides, under the test conditions used in this study. Regarding quantitative corrosion indicators, corrosion rates values (Table 3) obtained for A516 Gr70 indicated that this metal alloy was not suitable for a long-term design. It could be observed that coupons exposed to Solar_Salt_3%Cl mixture developed higher corrosion rates corroborating the important effect of chloride content in the corrosion damage over carbon steels.

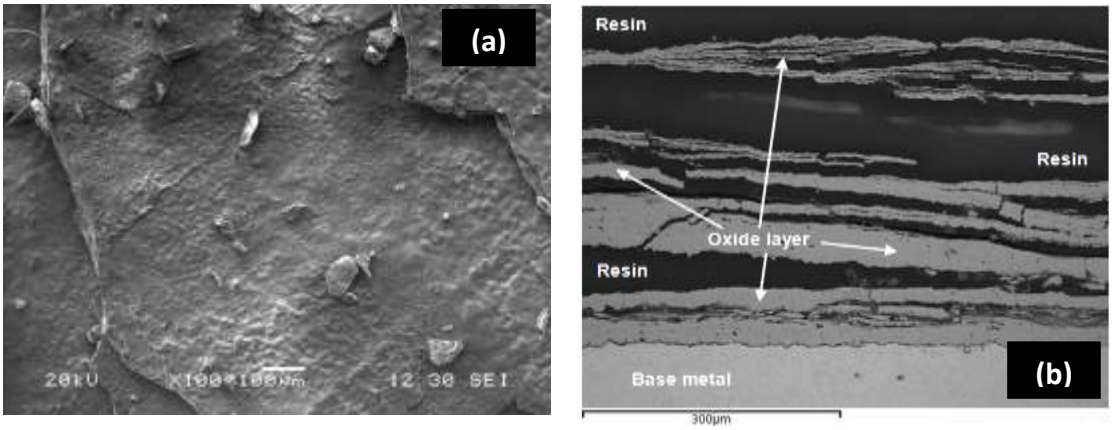

Figure 23. A516 Gr 70 coupons after exposition to Solar_Salt_3%Cl. a) Corrosion coupon surface SEM detail for coupon tested in Solar_Salt_3%Cl; b) Corrosion coupon transversal section SEM detail

Molten salt sample	Chloride content (%)	Weight gain (mg/cm^2)	Corrosion rate (µm/year)
Solar_salt_1.2%Cl	1.2	11.4	210
Solar_salt_3%Cl	3.0	38.5	535

Table 3. Corrosion damage quantitative indicators. Weight gain and corrosion rate

In conclusion, this study demonstrates the important role of chlorides in the corrosion mechanism of A516 Gr70 carbon steel. Chloride content increasing promotes the formation of thicker corrosion products and affects to the adherence between oxides layers and metal base. Moreover, iron oxides layers delamination and porosity avoid the formation of a compact and well adhered diffusion barrier not allowing the passivation of metal alloy. This phenomenon produces a synergic process accelerating the corrosion damage over the carbon steel. Then, solar salt mixtures with high chlorides content in the range of 1.2 to 3% by weight are not feasible for PTC applications considering current materials selection.

This study also provides a tentative materials selection to be used in TES system with high chlorides content nitrate salts. The cost reduction of using non-refined nitrates salts grades would allow the specification of more expensive metallic alloys with better corrosion resistance performance. However, the final materials selection should constitute an optimal compromise between technical and economic factors. CES

Selector software (Ashby approach) has been used to perform the proposed materials selection analysis [98, 99]. The starting point of the study was to establish the technical requirements of the metal alloy candidates. Then, constrains to take into account were as follow: (i) yield strength (260 MPa), (ii) tensile strength (485 MPa), (iii) service temperature (300 °C minimum), (iv) cost (< 10 €/kg), (v) corrosion resistance, (vi) easy manufacturing, and (vii) availability.

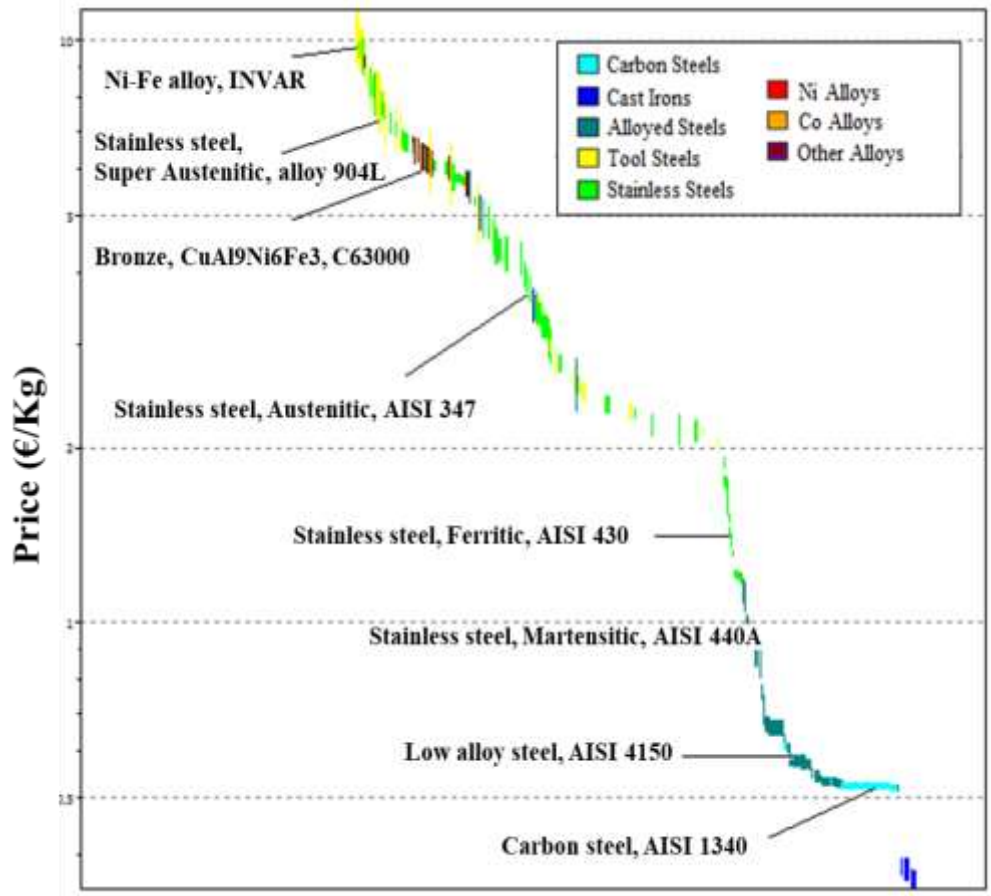

Figure 24. New materials selection. Metal alloys map for materials up to 10 €/kg

CES Selector outputs reveals that current materials selection could be replaced by higher corrosion resistant one being alloyed steels, martensitic stainless steels and ferritic stainless steels a first approach to be evaluated. The most interesting alloyed steels are focused on Cr-Mo alloyed steels, which are materials intended for high temperature and high-pressure vessels with Cr and Mo content in the range 0.03-9.5% and 0.35-1.10%, respectively. On the other hand, martensitic and ferritic stainless steels were selected as preliminary candidates as the most cost competitive alloys inside the stainless steels family (Cr content up to 18%). However, a detailed evaluation of the advantages and drawbacks for this application is needed for each candidate in a further study.

Finally, in addition to corrosion tests involving the new alloys candidates, a sensitivity study regarding extra cost produced by a more expensive materials selection and cost reduction associated to low purity nitrates salts is proposed prior to consider the use of use high chlorides content salts mixtures in commercial projects.

5.3. Contribution of the candidate

The candidate was in charge of the experimental-set up including the definition of the material to be tested, types of corrosion coupons, nitrates salts mixture qualities, test times, among others. Furthermore, the candidate defined the characterization to be performed over A516 Gr70 carbon steel coupons to evaluate the performance of this alloy after the exposition to both salt mixtures. The evaluation and discussion of the experimental results was also performed by the candidate. On the other hand, the evaluation of higher corrosion resistant candidates using CES Selector software was also carried out by the candidate obtaining three main alloys families to be analyzed in further studies. Finally, the candidate defined the structure of the paper and lead the writing process.

5.4. Journal Paper

Solar Energy Materials & Solar Cells 163 (2017) 134–147

Contents lists available at ScienceDirect

Solar Energy Materials & Solar Cells

journal homepage: www.elsevier.com/locate/solmat

Materials selection for thermal energy storage systems in parabolic trough collector solar facilities using high chloride content nitrate salts

F. Javier Ruiz-Cabañas[a,*], Cristina Prieto[a], Virginia Madina[b], A. Inés Fernández[c], Luisa F. Cabeza[d]

[a] Abengoa Research, C/ Energía Solar nº 1, Palmas Altas, 41014 Sevilla, Spain
[b] Materials for Energy and Environment Unit. Tecnalia Research and Innovation, Mikeletegi Pasealekua, 2, 20009 San Sebastián, Spain
[c] Department of Materials Science & Physical Chemistry, Universitat de Barcelona, Martí i Franqués 1-11, 08028 Barcelona, Spain
[d] GREA Innovació Concurrent, Universitat de Lleida, Edifici CREA, Pere de Cabrera s/n, Lleida, Spain

ARTICLE INFO

Keywords:
Corrosion
Carbon steel
A516 Gr70
Solar salts
Chlorides
Thermal energy storage (TES)

ABSTRACT

The increasing role of concentrated solar power (CSP) within the renewable energy portfolio is attributed to the possibility of integrating thermal energy storage (TES) systems. Then, CSP technology has become one of the most interesting clean options to deliver dispatchable power on demand. Nowadays, commercial facilities use high quality solar salts (60%:40% $NaNO_3$ and KNO_3 by weight) as storage medium due to the attractive properties of this fluid to be applied under CSP operation conditions. Taking into account that CSP installations are designed with really large TES systems containing tens of thousands of tons, the use of lower quality nitrates salts would reduce the molten salts inventory cost and finally the investment cost of the CSP storage systems at commercial scale. The most important drawback of selecting low quality nitrates salts for high temperature CSP applications is the corrosion impact produced by impurities. Accordingly, chlorides have been identified in the state of the art as the impurity with higher effect over corrosion. This work is focused on A516 Gr70 carbon steel corrosion performance evaluation under high-chlorides content nitrates salts (1.2% and 3% by weight) at 400 °C. In addition, the feasibility of using the proposed low purity mixtures with current CSP facilities materials selection is analyzed. Results reported within this study show the critical effect of chloride content over corrosion mechanism producing lack of adherence between base metal and oxides layers in addition to corrosion products delamination and internal cracking. Then, the use of A516 Gr70 carbon steel is rejected for a long term design under solar salts containing chlorides content in the range 1.2–3% by weight being necessary a higher corrosion resistant materials selection. An improved materials selection focused on higher corrosion resistance alloys is discussed.

Ruiz-Cabañas F.J., Prieto C, Osuna R., Madina V., Fernández A.I., Cabeza L.F. Materials selection for thermal energy storage systems in parabolic trough collector solar facilities using high chloride content nitrate salts. Solar Energy Materials And Solar Cells, 2017; 163: 134-147

https://doi.org/10.1016/j.solmat.2017.01.028

6. TES-PS10 Postmortem tests: Carbon steel corrosion performance exposed to molten salts under relevant operation conditions and lessons learnt for commercial scale-up

6.1. Introduction

Nowadays, the most mature configuration in the CSP sector is the parabolic PTC technology using thermal oil as HTF [100]. In this type of facilities, the thermal oil transfers its thermal energy to the steam, which is finally pumped to move the turbine of the installation to produce electricity. TES systems based on nitrates salts storage tanks are typically integrated in PTC CSP plants to adapt the electricity production to the energy demand [27]. One of the most important issues in the design of commercial TES systems is focused on performing an optimal materials selection of the different equipment and components in contact with nitrates salts. A wrong materials specification could result in a quick corrosion deterioration of the metal alloys used for the construction of the components. If the corrosion damage over the material is higher than the expected during the design phase, the facility would be subjected to important economic losses (facility repairs, loss of production, among others) and possible safety issues over the plant personnel [40, 41, 44, 45].

As detailed in the previous sections, the state-of-the-art shows that many authors have evaluated the corrosion performance of different alloys in contact with nitrate salts mixtures at different temperatures [46, 87-91]. Nevertheless, most of scientific contributions are focused on laboratory tests under controlled conditions. Accordingly, an important gap on reliable corrosion data obtained from studies performed under relevant operation conditions (commercial projects or large pilot plant facilities) is detected.

In addition to in-situ corrosion tests under relevant conditions (Paper 1 from this Thesis), postmortem evaluations become an interesting analysis to determine the status of materials after the shut-down of a facility once the lifetime of the plant has expired [101-104]. Then, postmortem tests are a powerful tool to validate the mechanical design of the installation, providing the following information in terms of corrosion:

- Corrosion performance of the selected materials under relevant operation conditions after thousands of operation hours

- Corrosion damages not detectable at laboratory scale due to difficulties to fully reproduce commercial operation conditions

- Feedback about materials selection and design guidelines to be used in future projects

The main goal of this manuscript is to perform a postmortem analysis based on components extracted from TES-PS10 pilot plant facility [34, 92]. Corrosion postmortem tests were performed after more than 30000 hours of operation under representative

commercial operation conditions. Several components of the installation were evaluated after the facility shut-down in order to characterize corrosion damage suffered by materials after the exposition to molten salts: (i) tank shell sections and (ii) molten salts pump sections (Figure 25). Two different tank shell sections (A516 Gr70) were extracted from both cold and hot storage vessels. Moreover, two sections were cut from the hot molten salts pump (discharge elbow and discharge pipe manufactured on ASTM A27 cast carbon steel) to analyze the corrosion performance of this component through which molten salts flow.

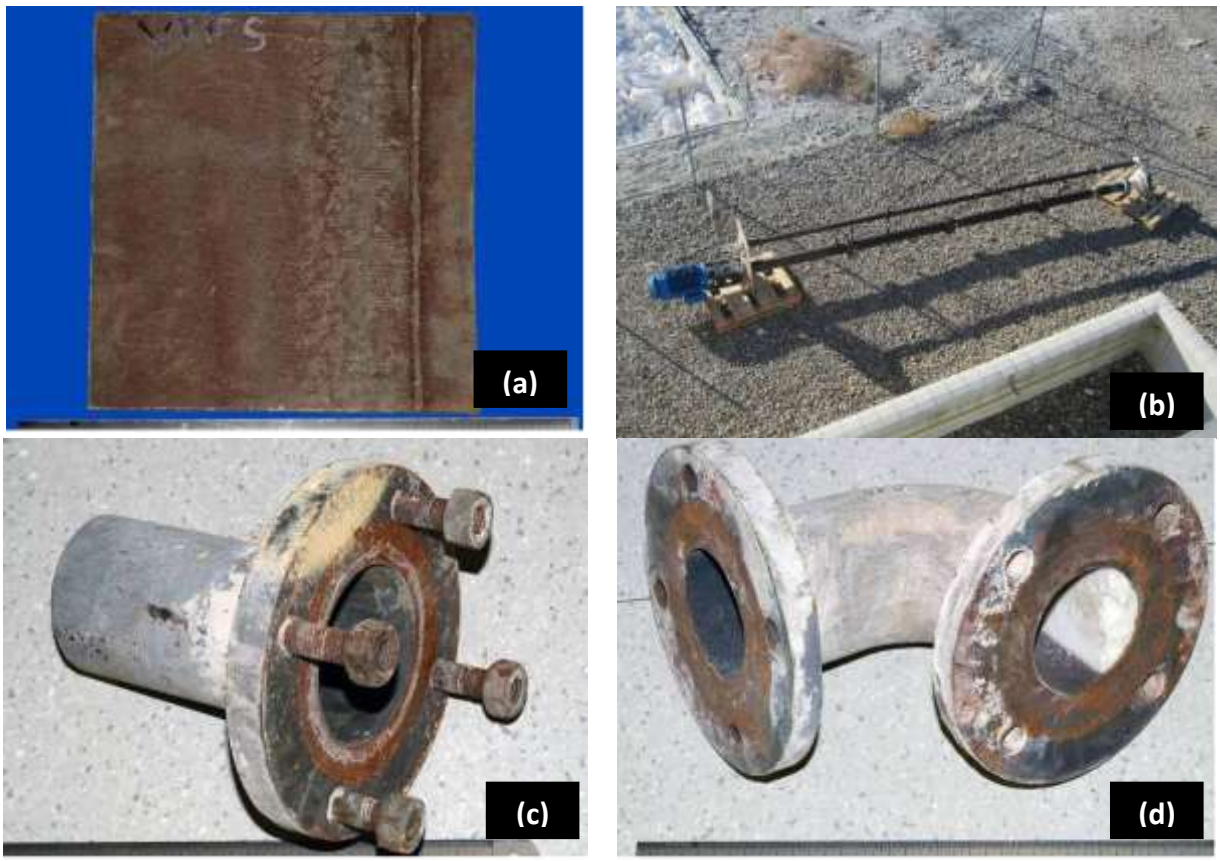

Figure 25. Components extracted from TES_PS10 pilot plant. a) Ferrule section removed from storage tank; b) Molten salts pump; c) Discharge pipe from molten salts pump; d) Discharge elbow from molten salts pump

Results obtained in this study provide understanding of corrosion performance of materials typically used for this application and lessons learnt to take into account for TES systems design to be integrated in PTC facilities at commercial scale.

6.2. Contribution to the state-of-the-art

This study covers the lack of information detected in the state-of-the-art about corrosion tests under relevant operation conditions. Specifically, the postmortem tests within this manuscript provides valuable information about the corrosion performance of metal alloys which are candidates for the construction of molten salts storage systems

in PTC CSP facilities. Then, results, conclusions and lessons learned extracted from the study are highly interesting for this field of knowledge because the operation conditions to which metal alloys were subjected are very similar to those of a commercial plant.

The characterization of the A516 Gr70 carbon steel shells sections showed some interesting findings not detected in previous studies performed in the same pilot plant using corrosion coupons (Paper 1). Firstly, the section cut from the upper section of the hot tank (UHT) displayed an exfoliating/delaminating non-protective oxide scale caused by breakaway corrosion phenomenon (Figure 26a). This attack appeared in the hot storage tank plates exposed to intermittent exposure due to the combination of CO_2, water vapor and chlorides at high temperature [105]. This mixture was in contact with carbon steel during the preheating of the vessel and later in the first weeks of operation when the preheating equipment was used as a back-up heating system. Secondly, all plates sections under evaluation (upper and lower shell sections for both tanks) developed small areas of localized corrosion barely penetrate through base metal (Figure 26 b). EDS spectra over this corrosion nodules confirmed the presence of chlorides being expected that Cl^- played an important role in the formation of this localized phenomena.

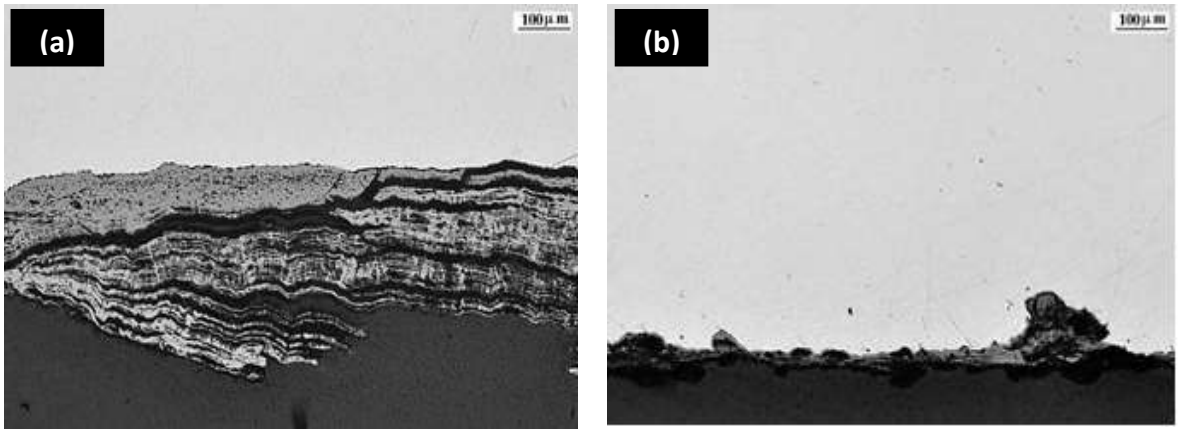

Figure 26. Ferrule sections micrograph. a), Oxide scale delamination in UHT shell plate section; b) Localized corrosion in UHT shell plate section

Both sections extracted from the hot salts pump (cast carbon steel) showed uniform corrosion developing adherent and quite uniform oxides layers. Moreover, corrosion-erosion phenomena due to molten salts pumping through this component were not detected. The microstructural characterization showed a really poor metallurgical quality of the cast steel due to the presence of many pores and cavities (Figure 27).

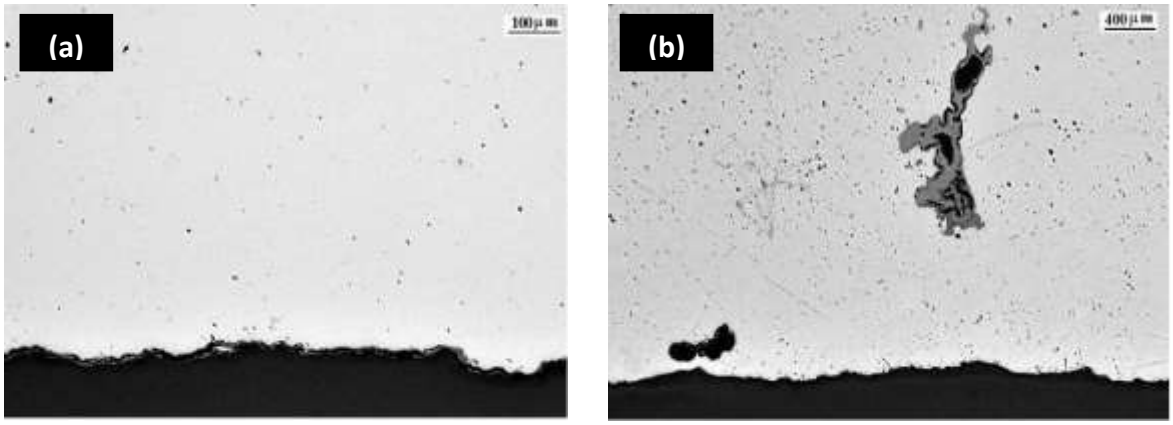

Figure 27. Pump sections micrographs. a) Discharge pump section internal surface cross section; b) Discharge Elbow cross section showing cavities

All the corrosion phenomena suffered by the components under evaluation could be corrected at commercial scale by applying the following lessons learned:

- The design of commercial preheating systems must assure a residual amount of CO_2 to be introduced during the preheating process avoiding the breakaway corrosion phenomenon

- Solar salts specification to be used in commercial projects must minimize the amount of chlorides avoiding two main drawbacks: (i) High corrosion rates due to nitrates salts corrosiveness is intimately related to chlorides percentage, and (ii) localized attack through base metal as analyzed within this study

- Exhaustive quality control must be performed over sections manufactured by casting processes to avoid in service failures

As conclusion, the materials selection analyzed within this postmortem evaluation is valid from corrosion point of view to be used in the design of commercial TES system using solar salts as storage fluid at temperatures in the range 290-390 °C.

6.3. Contribution of the candidate

The candidate was in charge of the corrosion postmortem test program selecting the components to be extracted from the TES-PS10 pilot plant. Moreover, the candidate defined the characterization to be performed over those metal sections to analyze the corrosion damage after more than 30000 hours exposed to molten salts. The candidate performed the evaluation and discussion of the results and led the writing of the manuscript. Furthermore, the candidate was responsible to compile all the lessons learned extracted from this study to consider them for commercial TES systems. Finally, the candidate developed the following specifications for commercial TES: Nitrates molten salts quality specification and Molten salts tanks preheating system specification.

6.4. Journal Paper

Journal of Energy Storage 26 (2019) 100922

Contents lists available at ScienceDirect

Journal of Energy Storage

journal homepage: www.elsevier.com/locate/est

TES-PS10 postmortem tests: Carbon steel corrosion performance exposed to molten salts under relevant operation conditions and lessons learnt for commercial scale-up

F. Javier Ruiz-Cabañas[a,*], Cristina Prieto[a,b], Virginia Madina[c], A. Inés Fernández[d], Luisa F. Cabeza[e]

[a] Abengoa Energía, Solar Technology department, Energía Solar 1, 41014 Sevilla, Spain
[b] Department of Energy Engineering, Universidad de Sevilla, Camino de los Descubrimiento s/n, 41092 Sevilla, Spain
[c] Materials and Processes Area, Tecnalia Research and Innovation, Mikeletegi Pasealekua, 2, 20009 San Sebastián, Spain
[d] Department of Materials Science & Physical Chemistry, Universitat de Barcelona, Martí i Franqués 1-11, 08028 Barcelona, Spain
[e] GREiA Research Group, INSPIRES Research Centre, Universitat de Lleida, Pere de Cabrera s/n, Lleida, Spain

ARTICLE INFO

Keywords:
Postmortem
Corrosion
TES-PS10
Solar salts
Carbon steel
Lessons learnt

ABSTRACT

Postmortem tests were performed over components removed from the TES-PS10 pilot plant after almost four years of continuous operation being exposed to solar salts under representative commercial operation conditions. Accordingly, corrosion performance of plates sections extracted from both storage tanks and samples cut from the hot molten salts pump were evaluated. Corrosion damage extension, oxides layers morphology, and corrosion products chemistry were analyzed by X-ray diffraction, energy dispersive X-ray spectrometry, optical microscopy, and SEM. In addition to materials compatibility with molten salts, mechanical tests were carried out over the storage tanks plates sections. Although the corrosion damage extension over the plates extracted from storage tanks was low and the mechanical properties were according to the standard, some interesting observations were seen. For example, a sample extracted from the hot storage tank and exposed to intermittent contact with molten salts showed some areas characterized by the growth of a non-protective oxide scale. Moreover, localized corrosion with slight penetration through the base material was identified for all storage plates samples under evaluation. On the other hand, the molten salt pump parts under study showed adherent and uniform oxides layers without detecting corrosion–erosion phenomena. Some cavities were found in the discharge elbow, and these imperfections were associated to a bad metallurgical quality during casting. Summarizing, corrosion phenomena suffered by the components under evaluation could be corrected in future plants by applying the lessons learned discussed in this study. As conclusion, materials selection analyzed within this postmortem evaluation is valid from the corrosion point of view to be used in the design of commercial TES systems in PTC plants.

Ruiz-Cabañas F.J., Prieto C., Madina V., Fernández A.I., Cabeza L.F. TES-PS10 postmortem tests: Carbon steel corrosion performance exposed to molten salts under relevant operation conditions and lessons learnt for commercial scale-up. Journal of Energy Storage, 2019; 26: 100922

https://doi.org/10.1016/j.est.2019.100922

7. Materials selection of steam-phase change material (PCM) heat exchanger for thermal energy storage systems in direct steam generation facilities

7.1. Introduction

One of the main emerging TES technologies within the thermosolar industry is the so-called PCM. The first advantage of those systems is the large energy density they have in comparison with systems working in the sensible region. The second interesting and peculiar characteristic is that PCM based systems deliver energy at constant temperature. This is an important difference regarding sensible heat solutions, which store and deliver energy while changing its temperature [15, 106-107].

PCM solutions have been usually related with DSG technology because their property of storing and delivering energy at a given temperature. Important efforts have been done trying to integrate the PCM technology within the DSG solar power generation. Feldhoff et al. [108] studied different alternatives to solve the TES system combining sensible and PCM subsystems (Figure 28).

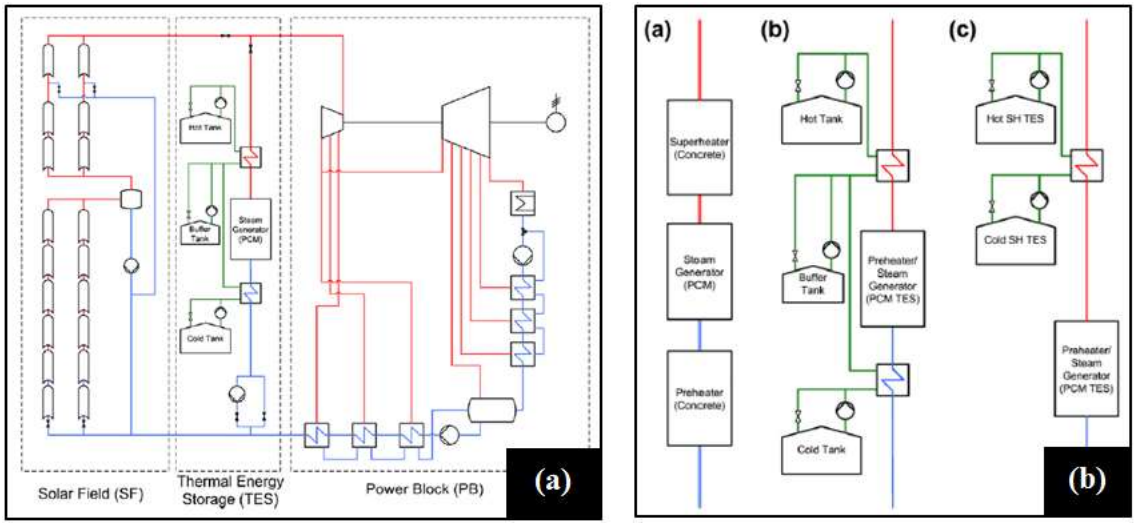

Figure 28. DSG plant configuration: a) Overall layout of DSG plant with TES system integrated, b) TES configurations alternatives for DSG technology [108]

An innovative configuration based on molten salt tanks and a PCM system was proposed within this manuscript to maximize the superheated steam discharge temperature using only two molten salt tanks and one PCM system [109, 110]. Different alternatives for PCM have been evaluated in the state of the art with melting temperatures able to cover power cycles around 120 bar. One of the most studied materials for those systems has been $NaNO_3$ with a melting point of 312 °C and an enthalpy change of 170 kJ/kg. On the other hand, some authors have been focused on different PCM solutions such as NaOH (77.2%wt) – NaCl (16.2%wt) – Na_2CO_3 (6.6%wt) mixture with a melting point of 318 °C and an enthalpy change of 290 kJ/kg [111].

This study is focused on a composite PCM based on an inorganic mixture of LiOH (46%wt) and KOH (54%wt) infiltrated in a high conductivity graphite foam [112]. LiOH-

KOH mixture has a melting point of 315 °C and an enthalpy change of 535 kJ/kg becoming this blend in one of the most interesting PCM media for DSG technology from the point of view of energy density and melting point. The heat is transferred between the LiOH-KOH mixture and steam in a shell and tube heat exchanger (Figure 29).

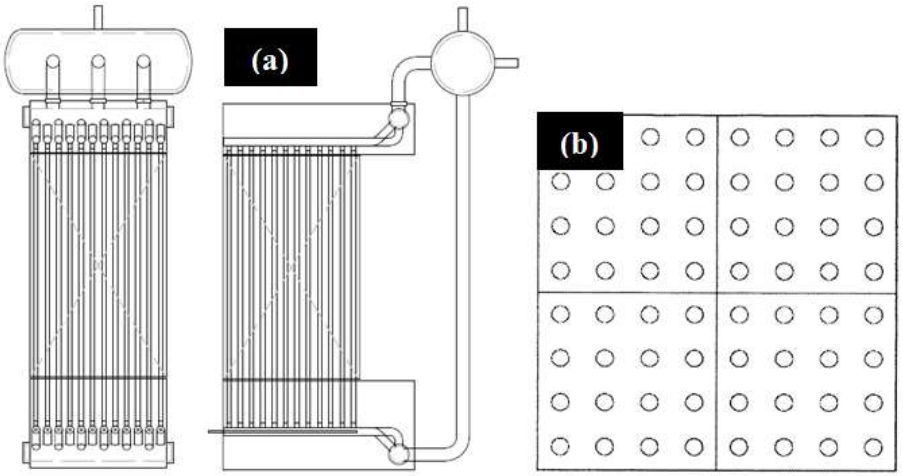

Figure 29. PCM heat exchanger: a) PCM heat exchanger sketch, b) Shell (PCM) & tubes [109, 110]

The scope of this manuscript is based on corrosion tests to identify a proper materials selection and associated corrosion allowance for the design of the PCM heat exchanger to be integrated in the TES system of the DSG facilities under discussion. Three different alloys, A516 Gr70 carbon steel, A316L stainless steel and Inconel 625 Ni-base alloy, were selected to validate the corrosion performance in contact with LiOH-KOH mixture at 360 °C.

7.2. Contribution to the state-of-the-art

Although extensive information regarding corrosion performance of metallic alloys in contact with steam has been reported in the state of the art, lack of knowledge has been detected concerning corrosion performance of selected LiOH-KOH mixture at the desired service temperature [83, 113-117]. In this way, results from this study cover this gap proposing a tentative materials solution to be used in the construction of the innovative Steam-PCM heat exchanger proposed for this application.

This study evaluates the corrosion performance of three alloys, A516 Gr70 carbon steel, A316L stainless steel and Inconel 625 Ni-base alloy, as container material for the construction of a high temperature heat exchanger for DSG technology. Different types of metallic coupons were assembled to corrosion racks to evaluate corrosion phenomena such as uniform corrosion, SCC, crevice corrosion, among others. In addition to corrosion rates calculation, SEM-EDS characterization was performed to evaluate the corrosion damage penetration in the alloy, oxides layers morphology and alloying elements evolution through corrosion products.

A516 Gr 70 showed the worst performance after testing in the hydroxide bath at 360 °C. In addition to high corrosion rates, corrosion products spallation was detected within the second test time. Therefore, iron oxides developed over metal alloys were not as protective as required to achieve full passivation and significant reduction in the corrosion rates after 2640 hours. However, localized corrosion phenomena such as pitting, SCC and crevice susceptibility were not detected for this carbon steel. Then, A516 Gr70 alloy is not recommended for the construction of the PCM heat exchanger.

A316L and Inconel 625 showed low corrosion rates, 6.3 and 15.2 µm/year respectively, being both materials suitable for this application. Protective and well adhered corrosion products, mainly composed by Fe, Ni and Cr, were identified for these alloys. Then, corrosion rates decreasing through exposure time is expected for these alloys. Although SCC and crevice corrosion susceptibility was not detected for both materials, slight corrosion progression through grain boundaries was displayed for A316L. Nevertheless, IGC attack depth was just limited to 10 µm depth.

Test time (hours)	A516 Gr70		A316L		Inconel 625	
	(mg/cm^2)	(µm/year)	(mg/cm^2)	(µm/year)	(mg/cm^2)	(µm/year)
t_1: 1005	-5.80	136	-0.07	10.3	0.30	30.0
t_2: 2640	-21.80	134	0.02	6.3	1.80	15.2

Table 4. Corrosion rates for A516 Gr70, A316L and Inconel 625

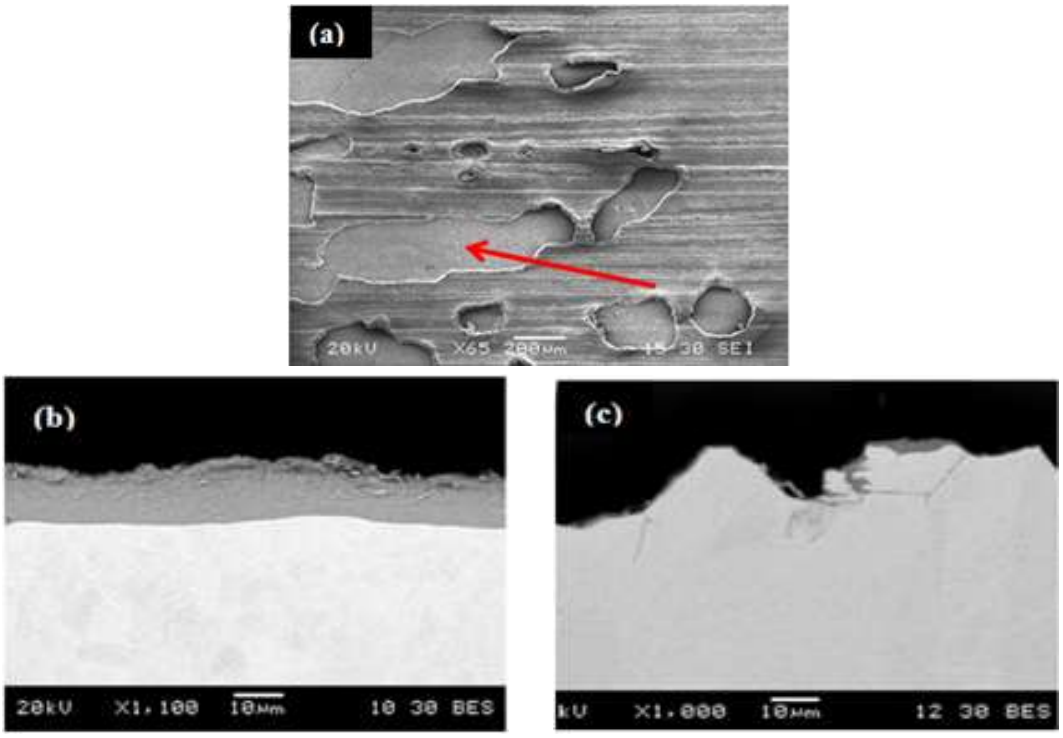

Figure 30. Coupons SEM characterization: a) A516 Gr70 after t2 test time; b) IN 625 after t2 time; c) A316L IGA detail

In conclusion, after a technical-economic feasibility study, A316L stainless steel is proposed as a first approach for the design of the steam-PCM heat exchanger. In addition to adequate thermal-mechanical properties and good weldability, this material displayed excellent corrosion performance during both test times. While A516 Gr70 was ruled out due to high corrosion rates and the development of non-protective oxide layers, Inconel 625 was discarded by cause of higher cost (6 times) and larger corrosion rates (2.4 times) than A316L.

Although a materials selection focused on stainless steel such as A316L optimizes the shell and tubes costs and thermal efficiency of the heat exchanger regarding Ni-base alloys, further detailed research would be required to analyze IGC phenomena detected after 2640 hours. Moreover, candidates such as Cr-Mo alloyed steels and ferritic stainless steels could be analyzed in a second step trying to optimize the design of the heat exchanger by using a more cost-effective materials selection.

7.3. Contribution of the candidate

The candidate developed the experimental-set up including the definition of the three material to be tested, types of corrosion coupons, test times, among other details. Furthermore, the characterization after testing to be performed over the different alloys was in charge of the candidate. The candidate carried out the evaluation and discussion of the experimental results identifying the proper candidate from technical-economical point of view. Moreover, the candidate proposed further tests to optimize the heat exchanger design using Cr-Mo alloyed steels and ferritic stainless steels as preliminary tentative candidates. Finally, the candidate defined the structure of the paper and led the writing process.

7.4. Journal Paper

Solar Energy Materials & Solar Cells 159 (2017) 526–535

Contents lists available at ScienceDirect

Solar Energy Materials & Solar Cells

journal homepage: www.elsevier.com/locate/solmat

Materials selection of steam-phase change material (PCM) heat exchanger for thermal energy storage systems in direct steam generation facilities

F. Javier Ruiz-Cabañas[a,*], Aleix Jové[a], Cristina Prieto[a], Virginia Madina[b], A. Inés Fernández[c], Luisa F. Cabeza[d]

[a] Abengoa Research, C/Energía Solar, 1, Palmas Altas, 41014 Sevilla, Spain
[b] Materials for Energy and Environment Unit, Tecnalia Research and Innovation, Mikeletegi Pasealekua, 2, 20009 San Sebastián, Spain
[c] Department of Materials Science and Physical Chemistry, Universitat de Barcelona, Martí i Franquès 1-11, 08028 Barcelona, Spain
[d] GREA Innovació Concurrent, Universitat de Lleida, Edifici CREA, Pere de Cabrera s/n, Lleida, Spain

ARTICLE INFO

Keywords:
Corrosion
Solar energy
Direct steam generation (DSG)
Thermal energy storage (TES)
Phase change material (PCM)
Hydroxides

ABSTRACT

Phase change materials (PCM) is one of the most interesting solutions to be used in thermal energy storage (TES) systems for direct steam generation (DSG) thermosolar facilities. Properties such as high energy density and energy storing/delivery at constant temperature bring PCM based systems in excellent candidates for DSG facility storage units. Accordingly, LiOH-KOH peritectic mixture, with a melting point of 315 °C and an enthalpy change of 535 kJ/kg, has been reported as attractive solution for the saturated storage module in DSG plants. A steam-PCM heat exchanger is the critical component to carry out the thermal transference between both substances. Although materials selection to be applied for steam applications is well known, lack of knowledge is detected in the field of high temperature hydroxides corrosion. Therefore, three metallic materials, A516 Gr70 carbon steel, A316L stainless steel and Inconel 625 Ni-base alloy, have been evaluated to determine their corrosion performance after hydroxides exposure. While A516 Gr70 was discarded for this application due to high corrosion rates, A316L and Inconel 625 displayed good corrosion resistance after 2640 h. Finally, A316L stainless steel was selected as potential candidate for the construction of the steam-PCM heat exchanger considering cost and thermal efficiency optimization.

Ruiz-Cabañas F.J., Jové A., Prieto C, Madina V., Fernández A.I., Cabeza L.F. Materials selection of steam-phase change material (PCM) heat exchanger for thermal energy storage systems in direct steam generation facilities. Solar Energy Materials And Solar Cells, 2017; 159: 526-535

https://doi.org/10.1016/j.solmat.2016.10.010

8. Steam-PCM heat exchanger design and materials optimization by using Cr-Mo alloys

8.1. Introduction

An optimized configuration based on molten salts tanks and PCM system has been proposed as TES module for DSG technology in the previous chapter. During periods without solar resource, sensible heat coming from molten salts is used for preheating and superheating the steam and latent heat is used for the evaporation process at constant temperature. While solar salt (60% $NaNO_3$-40%KNO_3) is used in the sensible storage module, an advanced PCM is proposed for the latent storage one [109, 110, 112]. The PCM solution is a composite based on a LiOH-KOH mixture (46wt.% and 54wt.%, respectively) infiltrated in graphite foam. The carbon structure is characterized by high volumetric thermal conductivity, low density, highly interconnected porosity, and relatively high stiffness. The significant properties of the LiOH/KOH mixture are: an interesting melting point for DSG applications, large amount of energy (535 kJ/kg as enthalpy change), fairly low relative volume expansion upon melting, and fairly low subcooling. Finally, the main advantages of the resulting composites are: very high energy density, relatively low volume expansion, highly enhanced heat transfer, stability, and insignificant hysteresis.

Thermal transference between steam and proposed PCM takes place in a shell and tubes heat exchanger where steam flows through the tubes and hydroxides-graphite foam composite freezes and melts inside the shell during charge and discharge operation modes. Previous chapter was focused on the evaluation of three different materials for the construction of the heat exchanger, A516 Gr 70 carbon steel, A316L stainless steel and Inconel 625 Ni base alloy (Paper 4 within this Thesis). The corrosion performance of these three materials was tested at laboratory scale. A316L austenitic stainless steel was preliminary selected as an interesting alloy for this application. However, the high cost associated to this material motivates the evaluation of low-cost alternatives to carry out a techno-economical optimization of the heat exchanger under discussion.

Within this chapter, ferritic stainless steels and Cr-Mo alloyed steels are proposed, as materials with an intermediate cost between carbon steels and austenitic stainless steels, for the heat exchanger optimization. Ferritic stainless steels consist of iron-chromium alloys. These materials have good ductility and formability but relatively poor high temperature strength compared to that of austenitic grades [118]. However, due to their lower chromium and nickel content, standard ferritic steel grades are usually less expensive than their austenitic counter-parts. On the other hand, chromium-molybdenum alloyed steels (A387 for plates and A335 for seamless pipes) are materials intended for high temperature and pressure services. Different grades of Cr-Mo alloyed steels are available, mainly attending to the amount of these alloying elements and the presence of small traces of V, Nb, N, Al, among others [119-121].

This study evaluates the corrosion behavior of A387 Gr91 alloy after exposition to the peritectic hydroxides mixture (LiOH-KOH) at different temperatures (315 and 360 °C).

8.2. Contribution to the state-of-the-art

Conclusions obtained within this manuscript contributes to the state-of-the-art providing the optimization of the Steam-PCM heat exchanger design proposed for the TES system in DSG CSP facilities. Then, a materials selection improvement is proposed regarding the one obtained in the previous chapter of this Thesis.

This study shows the main characteristics of two different alloys families such as ferritic stainless steels and Cr-Mo alloyed steels as candidates for the construction of the heat exchanger. Accordingly, typical application for these alloys, chemical compositions, mechanical properties, among other characteristics are discussed and compared. Finally, Cr-Mo alloyed steels have been selected to evaluate the corrosion performance after the exposition to LiOH-KOH peritectic mixture. Within this family, A387 Gr91 has been chosen as the alloy to be tested because of the following reasons: (i) Grade 91 shows the better mechanical performance within this family of alloys. (ii) The higher amount of Cr (8.00-9.50wt.%) associated to this alloy improve the corrosion resistance of this material regarding Cr-Mo alloys with lower Cr content, and (iii) the presence of Mo in the range of 0.85-1.05wt.% is also beneficial from a corrosion point of view [122].

Two different corrosion tests were proposed to evaluate the corrosion resistant of this alloy: Test#1, exposition at 360 °C and Test#2, exposition at 315 °C. A387 Gr 91 alloy generated compact and well adhered oxide layers after Test#1 not detecting localized corrosion damages (IGC, pitting or spalling phenomena). Moreover, X-Ray diffraction (XRD) spectrum identified CrO and $LiFeO_2$ as main oxides layers. The formation of lithium ferrate has been identified as a protective and passive oxide layer [123,124]. Some interesting characteristics associated to lithium ferrate regarding corrosion inhibition and protection are: (i) $LiFeO_2$ is insoluble in water, (ii) has a ceramics-like structure, and (iii) shows a high diffusion resistance to the migration of hydrogen, oxygen, iron and other atoms. Then, the formation of $LiFeO_2$ could be considered as beneficial in terms of corrosion to assure a good long-term performance.

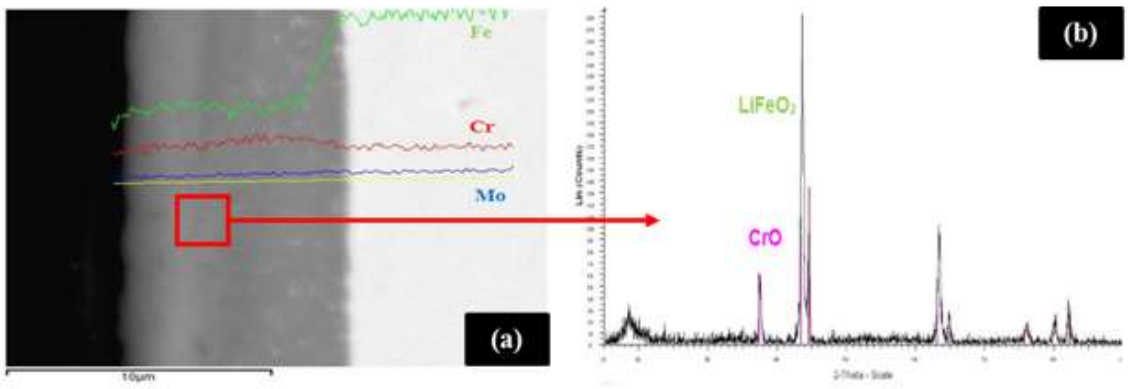

Figure 31. A387 Gr 91 SEM cross section micrographs: a) SEM micrograph and EDS profile (t1 test time, 1005 hours); b) XRD spectrum

Corrosion rates calculation corroborate the passivation of the alloy. In this way, corrosion rates decrease with the exposure time in the hydroxides bath. These results were compared with previous test on A316L alloy under same test conditions. A316L showed lower corrosion rates; 10.3 µm/year vs. 55.9 µm/year (t1 test time, 1005 hours) and 6.3 µm/year vs. 44.7 µm/year (t2 test time 2640 hours). Additional corrosion tests were carried out at 315°C to analyze the performance of A387 Gr91 at the exact process conditions in terms of temperature of the heat exchanger proposed for this application. Visual inspection and SEM analysis showed lower corrosion damage compared to Test#1. This observation was confirmed with corrosion rates calculation obtaining corrosion damage in the range of 29 µm/year after 1055 hours.

In addition to corrosion performance, other parameters such as cost, thermal properties, and mechanical properties have been discussed within this study. A387 gr 91 cost is lower than A316L ones due to the lower content of Ni, Cr, and Mo. Moreover, A387 Gr91 thermal conductivity is higher, which is a key point for the thermal transference between the PCM and steam. On the other hand, A387 Gr 91 maximum allowable stresses (MAS) values are also significantly higher. The better mechanical performance has a direct impact on the sizing of the equipment reducing the thickness required for the temperature and pressure combination.

In conclusion, A387 Gr91 is a more promising alloy for the manufacturing of the steam-PCM heat exchanger than A316L alloy. Although corrosion rates obtained for A387 Gr91 are higher, passivation of the alloy has been demonstrated and good long-term corrosion performance is expected. Moreover, IGC damage has not been detected for A387 Gr 91, which is one of the main drawbacks found for A316L. On the other hand, properties such as thermal conductivity, MAS, and cost of the alloy make this material a better candidate for this application.

8.3. Contribution of the candidate

The candidate was in charge of the evaluation of new alloys for the construction of the Steam-PCM heat exchanger. He checked the properties of both alloys' families analyzing main advantages and drawbacks finally selecting the A387 Gr91 alloyed steel for corrosion testing. The definition of the corrosion test matrix was led by the candidate defining tests temperatures, corrosion coupons, tests times and characterization to be executed after the exposition to hydroxides bath. The candidate also performed the evaluation and discussion of the experimental results. Moreover, the candidate performed the comparison of A387 Gr91 and A316L alloys including parameters such as conductivity, thermal-mechanical properties, cost and final design of tubes. Finally, the candidate defined the structure of the paper and led the writing process.

8.4. Journal Paper

Solar Energy Materials and Solar Cells 178 (2018) 249–258

Contents lists available at ScienceDirect

Solar Energy Materials and Solar Cells

journal homepage: www.elsevier.com/locate/solmat

Steam-PCM heat exchanger design and materials optimization by using Cr-Mo alloys

F. Javier Ruiz-Cabañas[a,*], Cristina Prieto[a], Aleix Jové[a], Virginia Madina[b], A. Inés Fernández[c], Luisa F. Cabeza[d]

[a] Abengoa Research, C/ Energía Solar nº 1, Palmas Altas, 41014 Sevilla, Spain
[b] Materials for Energy and Environment Unit. Tecnalia Research and Innovation, Mikeletegi Pasealekua, 2, 20009 San Sebastián, Spain
[c] Department of Materials Science & Physical Chemistry, Universitat de Barcelona, Martí i Franquès 1-11, 08028 Barcelona, Spain
[d] GREiA Research Group, INSPIRES Research Centre, Universitat de Lleida, Pere de Cabrera s/n, Lleida, Spain

ARTICLE INFO

Keywords:
Corrosion
Phase change material (PCM)
Cr-Mo alloys
Hydroxides
Thermal energy storage (TES)

ABSTRACT

A387 Gr 91 Cr-Mo alloy corrosion compatibility with LiOH-KOH mixture was evaluated at 315 °C (Test#1) and 360 °C (Test#2). This alloy is studied for a techno-economical optimization of a steam-PCM heat exchanger proposed in the thermal energy storage (TES) system of a direct steam generation (DSG) facility. The corrosion damage was analyzed with visual inspection, optical microscopy, SEM, EDS and XRD, and corrosion rates were also calculated. A387 Gr 91 alloy generates protective oxide layers over base metal. Localized corrosion damages were not detected with these test conditions, while XRD and EDS profiles showed CrO and $LiFeO_2$ as main corrosion products generated by this alloy. On the other hand, corrosion rates decrease with exposure time showing the passivation of the alloy. A387 Gr 91 corrosion performance was compared with A316L stainless steel, which was preliminary proposed by the authors in previous studies. In addition to corrosion performance, parameters such as cost, thermal properties, and mechanical properties are discussed. In conclusion, the use of A387 Gr 91 instead to A316L alloy for the construction of the steam-PCM heat exchanger involves the techno-economical optimization of the equipment.

Ruiz-Cabañas F.J., Prieto C, Jové A., Madina V., Fernández A.I., Cabeza L.F. Steam-PCM heat exchanger design and materials optimization by using Cr-Mo alloys. Solar Energy Materials And Solar Cells, 2018; 178: 249-258

https://doi.org/10.1016/j.solmat.2018.01.038

9. Conclusions and recommendations for future work

9.1. Conclusions of the thesis

This thesis contributes to broaden the knowledge in the field of corrosion associated to inorganic salts used in TES systems for CSP facilities. The compatibility between metal alloys and inorganic salts has been evaluated for two different storage modules. On the one hand, corrosiveness of solar salts (60% $NaNO_3$-40% KNO_3) used in sensible double-tank storage systems integrated in PTC plants has been analyzed at two scales: Pilot plant and laboratory. On the other hand, LiOH-KOH peritectic mixture corrosivity has been tested to identify a proper materials selection for the construction of a Seam/PCM heat exchanger. This heat exchanger is the key component of the latent heat thermal storage module proposed within this Thesis for DSG CSP installations.

Main conclusions and achievements obtained from in-situ corrosion tests launched in the storage tanks of the TES-PS10 pilot plant facility using corrosion racks are as follow:

- A CTD has been successfully designed following the ASTM standard guidelines. This tool allows the evaluation of corrosion phenomena inside thermal storage tanks in operation. Moreover, the CTD is durable, inexpensive and has no maintenance during the life of the project. Finally, both procedures, the assembly of the CTD to the storage tanks and the CDT removal after the different test times are easy to carry out on site

- A516 Gr70 corrosion coupons (same material as TES-PS10 storage tanks) shows an excellent corrosion performance after the exposition to solar salts at 390°C during more than 8000 hours

- Corrosion rates for both expositions to nitrates salts, continuous and intermittent, were quite low. While corrosion rates associated to continuous exposition was 2.14 µm/year after 8712 hours, 3.57 µm/year were measured for the intermittent one. Moreover, the exposition to molten salts is more aggressive that alternative exposure to salts and nitrogen

- Oxides layers generated over the base metal were compact and well adhered for all test times and expositions. Spalling phenomena or other localized damages such as pitting corrosion, IGC, among others were not found during the inspection of coupons surface and cross sections by optical microscopy and SEM

- Corrosion rates decreased with the exposure time to nitrates salts going from 22.14 µm/year after 1680 hours down to 2.14 µm/year at 8712 hours. Then, the corrosion damage evolution confirmed the passivation of the carbon steel expecting low/negligible corrosion rates for longer times

- A516 Gr70 carbon steel is highly recommended for the construction of commercial molten salts tanks in TES systems at temperatures up to 390°C. The

selection of this alloy assures a long-term design due to low corrosion damage is expected for the lifetime of a commercial project

- Outputs from this study were used to prepare several technical specifications to be applied in commercial projects summarizing the lessons learned obtained from these tests:

  1) Molten salts storage tanks materials specification for PTC plants

  2) Molten salts storage tanks corrosion allowances specification for PTC plants

  3) Corrosion preventive maintenance of molten salts storage tanks by using CTD

Regarding the corrosion evaluation of high chlorides content solar salts, the main outputs of the study are:

- Corrosion rates measured over A516 Gr70 carbon steel after the exposition to both mixtures are high. While 210 µm/year corrosion rate was obtained for samples submerged in Solar_Salt_1.2%Cl mixture, 535 µm/year was measured for the higher chloride content nitrates mixture (Solar_Salt_3%Cl) after 1581 hours

- In addition to high corrosion rates, oxides layers developed over base metal were not adherent and protective. The presence of chlorides promotes the porosity of the scales and finally the spalling of these oxides. Then, it is not possible to obtain the passivation and therefore it is not expected a corrosion rates reduction for longer times

- Solar salt mixtures with high chlorides content in the range of 1.2 to 3% by weight are not feasible for PTC applications considering current alloys, A516 Gr70 carbon steels for tanks and steels with similar chemical compositions for piping

- The use of high chlorides content nitrates salts (1.2 to 3%) in TES systems integrated in PTC facilities requires a new materials selection with a higher corrosion resistant performance

- Ashby methodology is a useful tool for carrying out a systematic approach to solve the materials selection of complex systems. Then, CES Selector software provides a starting point for the selection of new candidates for the construction of equipment and components of a TES system using solar salts with high chlorides content

- Cr-Mo alloyed steels and martensitic and ferritic stainless steels are preliminary proposed to replace current materials selection. Cr-Mo alloyed steels are typical alloys used for high-pressure vessels with Cr and Mo content in the range of 0.03-9.5% and 0.35-1.10%, respectively. On the other hand, ferritic and martensitic

steels are also selected as low-cost options inside the stainless steels families due to absence of Ni in their compositions

- In addition to specific corrosion tests, it is needed a deep analysis of the new proposed alloys including advantages and disadvantages of each material, construction requirements, materials costs, corrosion performance in similar environments, among others. Finally, a sensitivity study between costs associated to new materials selection, alloys performance and cost savings due to the use of low purity solar salts is needed to consider the use of high chlorides content salts mixtures in commercial projects

Regarding the postmortem tests carried out over several components of the TES-PS10 pilot plant after the shut-down of the facility, main interesting conclusions are as follow:

- Postmortem tests are a powerful tool to analyze the status of the different equipment and components of an industrial plant after the definitive shut-down of such facility

- Following information could be obtained from postmortem tests regarding corrosion performance of the materials used in the plant:

  1) To analyze the corrosion performance of materials selection under real operation conditions

  2) To identify possible corrosion damages not detectable at laboratory scale due to difficulties to reproduce commercial operation conditions

  3) To obtain feedback about materials selection and design guidelines to be used in commercial projects

- A516 Gr70 carbon steel shells sections extracted from molten salts storage tanks showed some corrosion phenomena not detected in previous in-situ corrosion tests using CTD

- Hot tank upper section developed breakaway corrosion phenomena generating oxides layers, which easily delaminates from the base metal. This damage was produced by the tank preheating system, which introduced a non-controlled amount of CO_2 inside the tanks. Then, carbon steel shells were exposed in the hot tank to a mixture composed by CO_2, water vapors and chlorides at high temperature producing this type of attack

- All plates sections (hot and cold tank, upper and lower sections) displayed small corrosion nodules, which penetrates through the base metal. Chlorides were detected in these areas after checking EDS spectra. Then, it is expected that

chlorides promoted the formation of such localized attack after the exposition of the material to nitrates salts during more than 30000 hours

- Pumps sections showed cast imperfections such as pores and cavities. However, these sections displayed low corrosion attack over the material developing thin and well adhered oxides layers

- All previous corrosion phenomena are avoidable at commercial scale applying the following lessons learned:

  1) Tanks preheating system specification shall require that the amount of CO_2 introduced in the TES system is close to zero

  2) Solar salts chemical composition specification shall minimize the amount of chlorides as impurity in the nitrates supplied by the vendors

  3) Exhaustive quality control supervision for all the components and equipment to be used in the TES systems

Finally, conclusions obtained from the materials selection analysis for the latent heat TES module proposed for DSG CSP facilities are as follow:

- A Steam/PCM heat exchanger is presented for the evaporation TES module. This component is a shell & tubes heat exchanger where steam flows through the tubes while PCM melts and freezes depending on the operation mode of the system (charge/discharge)

- A composite PCM is proposed to be integrated in such heat exchanger to transfer the thermal energy with the water/steam during the operation of the TES module. This composite PCM consists of a graphite matrix into which a peritectic mixture of hydroxides (46% LiOH - 54% KOH) is infiltrated. Properties associated to this composite PCM are high conductivity, enthalpy change of 535 kJ/kg and melting point in the range of 315 °C

- Three different alloys were preliminary selected to evaluate their corrosion resistant to the hydroxide mixture; A516 Gr70 carbon steel, A316L austenitic stainless steel and Inconel 625 Ni-base alloy

- A516 Gr70 carbon steel showed the worst corrosion performance developing spalling phenomena in the oxides layers in addition to high corrosion rates (134 µ/year after 2640 hours). On the other hand, stainless steel and Ni-base alloy displayed low corrosion rates, 6.3 and 15.2 µm/year respectively. Moreover, corrosion rates for these two alloys decreased with exposure time which mean that base material is being passivated by the oxides layer generated during the exposure to hydroxides bath

- A316L was preliminary selected for the construction of the shell and tubes heat exchanger. Reasons for the selection of this alloy instead Inconel 625 were the lower corrosion rates and lower cost regarding to the Ni-base alloy. However, the slight IGC damage observed for A316L should be evaluated more in detail in further studies

- Additional corrosion tests were developed to optimize from technical-economical point of view the materials selection of the Steam/PCM heat exchanger. In this way, A387 Gr91 (Cr-Mo alloyed steel with Cr and Mo in the range of 8.00-9.50wt.% and 0.85-1.05wt.% respectively) was selected for corrosion testing. Properties such as good weldability, mechanical properties, cost and corrosion resistant become this alloy as a promising material for the construction of this component

- Corrosion rates measured over A387 Gr91 coupons were 44.7 µm/year at 360°C after 2640 hours and 29 µm/year at 315°C after 1055 hours. In addition to relative low corrosion rates, reduction in the corrosion rates were detected with the exposure time. Moreover, lithium ferrate ($LiFeO_2$) was detected in the corrosion products. This oxide layer has been identified as a protective and passive oxide layer in other environments providing a diffusion barrier resistance to the migration of hydrogen, oxygen, iron and other atoms

- Corrosion rates associated to A387 Gr91 are higher than A316L ones. However, the better performance on thermal conductivity, mechanical properties (MAS) and lower cost, becomes this alloy as attractive alternative to austenitic stainless steels for the construction of the Steam/PCM heat exchanger

9.2. Recommendations for future works

From the research carried out and presented in this thesis, some points arise which are not addressed within this study and are relevant in the field of corrosion associated to inorganic salts used in TES systems for CSP plants. Recommendations for further works are listed below:

- To evaluate the corrosion performance of metal alloys used for the construction of commercial TES systems integrated in PTC facilities. In-situ corrosion campaigns using the CTD designed within this Thesis would be proposed. Results would be compared with the ones obtained within this Thesis at laboratory and pilot plant scale

- To perform in-situ corrosion tests in CSP molten salts tower plants. Although there are many studies about the corrosion behavior of different types of alloys exposed to solar salts at temperatures in the range of 500-600 °C, lack of information is detected about tests carried out in relevant operation conditions. A complete corrosion test program is as follow:

- Introduction of CTD in the cold tank of the facility assembling carbon steel coupons. In this way, a possible corrosion aggressiveness increasing due to thermal degradation of solar salts will be evaluated in the cold side of the installation

- Introduction of CTD in the hot tank of the TES system. Corrosion coupons under evaluation could be different types of stainless steels and Ni-base alloys. Final materials selection to be tested would be performed by the researcher taking into account alloys used in the construction of the hot side of the installation and also promising candidates found in the literature. Results obtained from these tests at commercial scale would be compared with the ones reported in the state of the art

- In addition to test campaigns in the molten salts tanks, corrosion racks could be also installed in the piping system of the plant. Then, corrosion-erosion phenomena over the metal alloys produced by the nitrates salts flow could be analyzed for both pipelines, cold and hot at temperatures of 300 and 565 °C respectively. Results would be compared with the state of the art and also with conclusions obtained from coupons extracted from the storage tanks

10. Others research activities

10.1. Other publications

- Prieto C., Gallardo-González J., Ruiz-Cabañas F.J., Barreneche C., Martínez M., Segarra M., Fernández A.I. Study of corrosion by Dynamic Gravimetric Analysis (DGA) methodology. Influence of chloride content in solar salt. Solar Energy Materials and Solar Cells, 2016; 157: 526-532

- Prieto C, Ruiz-Cabañas FJ, Rodríguez-Sánchez A, Rubio C, Fernández AI, Martínez M, Oró E, Cabeza LF. Effect of the impurity magnesium nitrate in the thermal decomposition of the solar salt. Solar Energy, 2019; 192:186-192

- Prieto, C., Rodríguez-Sánchez, A., Ruiz-Cabañas, F.J., Cabeza, L.F. Feasibility study of freeze recovery options in parabolic trough collector plants working with molten salt as heat transfer fluid. Energies, 2019; 12: 2340

- Prieto C., Fereres S., Ruiz-Cabañas F.J., Rodriguez-Sanchez A., Montero C. Carbonate molten salt solar thermal pilot facility: Plant design, commissioning and operation up to 700 °C. Renewable Energy, 2020; 151: 528-541

11. References

[1] Siva V, Kaushik S, Ranjan K, et al. State-of-the-art of solar thermal power plants: A review. Renewable and Sustainable Energy Reviews, 2016; 54: 1085–1091

[2] Jebasingh VK, Joselin Herbert GM. A review of solar parabolic trough collector. Renewable and Sustainable Energy Reviews, 2016

[3] Abbas R, Muñoz-Antón J, Valdés M, et al. High concentration linear Fresnel reflectors. Energy Conversion and Management, 2013; 72: 60-68.

[4] Behar O, Khellaf A, Mohammedi K. A review of studies on central receiver solar thermal power plants. Renewable and Sustainable Energy Reviews, 2013; 23: 12-39

[5] Kongtragool B, Wongwises S. A review of solar-powered Stirling engines and low temperature differential Stirling engines. Renewable and Sustainable Energy Reviews, 2003, 7: 131-154

[6] Purohit I, Purohit P, Shekhar S. Evaluating the potential of concentrating solar power generation in North western India. Energy policy, 2013; 62: 157-175

[7] Dinçer I, Rosen M. Thermal energy storage systems and applications. Second Edition. A John Wiley and Sons, Ltd.

[8] Laing D, Steinmann W, Tamme R, et al. Solid media thermal storage for parabolic trough power plants. Solar Energy, 2006, 80: 1283-1289

[9] Vignarooban K, Xu X, Arvay A, Hsu K, Kannan AM. Heat transfer fluids for concentrating solar power systems – A review. Applied Energy, 2015; 146: 383-396

[10] Kearney D, Herrmann U, Nava P, et al. Assessment of a Molten Salt Heat Transfer Fluid in a Parabolic Trough Solar Field. Journal of solar energy engineering, 2003; 125: 170-176

[11] Sena-Henderson L. Advantages of using molten salts, national solar thermal test facilities. SANDIA National laboratories 2006.

[12] Gomez JC, Calvet N, Starace AK, Glatzmaier GC. $Ca(NO3)_2$–$NaNO_3$–KNO_3 molten salt mixtures for direct thermal energy storage systems in parabolic trough plants. Journal of Solar Energy Engineering-ASME 2013; 135:021016

[13] Olivares RI, Edwards W. $LiNO_3$–$NaNO_3$–KNO_3 salt for thermal energy storage: thermal stability evaluation in different atmospheres. Thermochimica Acta, 2013; 560: 34–42

[14] Fernandez AG, Ushak S, Galleguillos H, Perez FJ. Development of new molten salts with $LiNO_3$ and $Ca(NO_3)_2$ for energy storage in CSP plants. Applied Energy 2014; 119: 131–40

[15] Prieto C, Cabeza LF. Thermal energy storage (TES) with phase change materials (PCM) in solar power plants (CSP). Concept and plant performance. Applied Energy, 2019; 254: 113646

[16] Zalba B, Marín JM, Cabeza LF, Mehling H. Review on thermal energy storage with phase change: materials, heat transfer analysis and applications. Applied thermal engineering, 2003; 23: 251–83

[17] Do Couto Aktay K, Tamme R, Müller-Steinhagen H. Thermal Conductivity of High-Temperature Multicomponent Materials with Phase Change. International Journal of Thermophysics, 2008, 29: 678-792

[18] Lane GA. Solar heat storage: latent heat material, volume II: technology. CRC Press, Inc

[19] Tamme R. The DISTOR project consortium–objective–achievements. DISTOR dissemination workshop ‘‘Energy Storage for Direct Steam Solar Power Plants’’, 2007, PSA Almeria, Spain

[20] Pardo, P, Deydier, A, Anxionnaz-Minvielle, Z, et al. A review on high temperature thermochemical heat energy storage. Renewable and Sustainable Energy Reviews, 2014, 32: 591-610

[21] Prieto C, Cooper P, Fernández AI, Cabeza LF. Review of technology: Thermochemical energy storage for concentrated solar power plants. Renewable and Sustainable Energy Reviews, 2016; 60: 909-929

[22] Van Berkel J. Storage of solar energy in chemical reactions. Thermal energy storage for solar and low energy buildings. 2005, Lleida, Spain

[23] Gil T, Medrano M, Martorell I, Lázaro A, Dolado P, Zalba B, Cabeza LF. State of the art on high temperature thermal energy storage for power generation. Part 1 Concepts, materials and modelization. Renewable and Sustainable Energy Reviews, 2010; 14: 31-55

[24] Zhanga H, Baeyens J, Degréve J. Concentrated solar power plants: Review and design methodology. Renewable and Sustainable Energy Reviews, 2013; 22: 466–481

[25] Herrmann U, Geyer M, Kearney D. Overview on thermal storage systems. Workshop on Thermal Storage for Trough Power Plants. FLABEG Solar International GmbH, 2006

[26] http://greenterrafirma.com/solar-thermal-for-electricity.html (Accessed July 2020)

[27] Herrmann U, Kelly B, Price H. Two-tank molten salt storage for parabolic trough solar power plants. Energy, 2004, 29: 883–893.

[28] Brosseau D, Kelton J, Ray D, et al. Testing of thermocline filler materials and molten-salt heat transfer fluids for thermal energy storage systems in parabolic trough power plants. Journal of solar energy engineering, 2005, 127: 109–116

[29] Emerson J Micah H, Panneer S. Concrete as a thermal energy storage medium for thermocline solar energy storage systems. Solar Energy, 2013; 96: 194–204

[30] Salomonia V, Majoranaa C, Giannuzzib G, et al. Thermal storage of sensible heat using concrete modules in solar power plants. Solar Energy, 2014; 103: 303-315

[31] Bauer T, Pfleger N, Laing D, et al. Molten Salts Chemistry From Lab to Applications. Chapter 20: High-Temperature Molten Salts for Solar Power Application, 415-438, Elsevier Inc

[32] Curso sistemas solares de concentración. Capítulo 3: Tecnologías de almacenamiento térmico para SSC - 2. León J. 2006, Centro de investigaciones energéticas, medioambientales y tecnológicas (CIEMAT)

[33] Winter C, Sizmann R, Vant-Hull L. Solar power plants. Chapter 6: Thermal storage for solar power plants. Springer-Verlag Berlin Heidelberg New York

[34] http://www.abengoa.es/htmlsites/boletines/en/abril2010/solar.html (Accessed July 2020)

[35] Reilly H, Kolb G. An evaluation of molten salt power towers including results of the Solar Two project, 2001, SANDIA National laboratories, SAND2001-3674

[36] https://www.energy.gov/lpo/solana (Accessed July 2020) (Accessed July 2020)

[37] https://cerrodominador.com/en/home-en/ (Accessed July 2020) (Accessed July 2020)

[38] Bayón R, Rojas E, Valenzuela L, Zarza E, León J. Analysis of the experimental behaviour of a 100 kWth latent heat storage system for direct steam generation in solar thermal power plants. Applied Thermal Engineering, 2010; 30: 2643-2651

[39] Laing D, Bahl C, Bauer T, Lehmann D, Steinmann WD. Thermal energy storage for direct steam generation. Solar Energy, 2011; 85: 627-633

[40] El-Meligi A. Corrosion Preventive Strategies as a Crucial Need for Decreasing Environmental Pollution and Saving Economics. Recent Patents on Corrosion Science, 2010, 2: 22-33

[41] Koch G, Brongers M, Tompson N, et al. Corrosion costs and preventive strategies in the United States, NACE 2002, Publication: FHWA-RD-01-156

[42] Trethewey KR, Chamberlain J. Corrosion for science and engineering. 2nd ed. New York: Longman Group Limited 1995

[43] Bhaskaran R, Palaniswamy N, Rengaswamy N, et al. ASM Hand Book vol 13B (ASM International, Metals Park, Ohio), 2005

[44] Elayaperumal K, Raja VS. Corrosion failures: Theory, case Studies, and solutions. 2015 Willey Series in Corrosion

[45] Bardal E. Corrosion and protection. Engineering materials and processes, Springer-Verlag London. 2004

[46] Walczak M, Pineda F, Fernández AG, Mata-Torres C, Escobar RA. Materials corrosion for thermal energy storage systems in concentrated solar power plants. Renewable and sustainable energy reviews, 2018; 86: 22-44

[47] ASTM G1-03. Standard practice for preparing, cleaning and evaluating corrosion test specimens, ASTM International

[48] Picture showing uniform corrosion of carbon steel exposed to nitrates salts. Abengoa internal research activities

[49] Matjaž F. Galvanic series of different stainless steels and copper and aluminum-based materials in acid solutions. Corrosion Science, 2013, 68: 51–56

[50] https://www.structuremag.org/?p=9609 (Accessed July 2020)

[51] Sharland S. A review of the theoretical modeling of crevice and pitting corrosion. Corrosion Science, 1987, 27: 289-323

[52] Dayal R. Corrosion of austenitic stainless steels, mechanism, mitigation and monitoring. Chapter IV: Crevice corrosion of stainless steels. Woodhead Publishing Limited, 2002

[53] Hu Q, Zhang G, Qiu Y, et al. The crevice corrosion behavior of stainless steel in sodium chloride solution. Corrosion Science, 2011, 53: 4065–4072

[54] http://www.substech.com/dokuwiki/doku.php?id=crevice_corrosion (Accessed July 2020)

[55] http://www.cdcorrosion.com/mode_corrosion/corrosion_crevice.htm (Accessed July 2020)

[56] Schweitzer P. Fundamentals of corrosion, mechanisms, causes and preventive methods. CRC press, Taylor and Francis Group, LLC, 2010

[57] http://www.substech.com/dokuwiki/doku.php?id=pitting_corrosion (Accessed July 2020)

[58]https://www.neonickel.com/technical-resources/general-technicalresources/pitting-corrosion/ (Accessed July 2020)

[59] Engelberg D. Shreir's Corrosion, Volume 2: Corrosion in Liquids, corrosion evaluation. Chapter VI: Intergranular Corrosion. Elsevier, 2010

[60] Yae A, Souza V, Tavares S, et al. Influence of heat treatments on the intergranular corrosion resistance of the AISI 347 cast and weld metal for high temperature services. Journal of Materials Processing Technology, 2008, 199: 391–395

[61] Terada M, Escriba D, Costa I, et al. Investigation on the intergranular corrosion resistance of the AISI 316L(N) stainless steel after long time creep testing at 600 °C. Materials Characterization, 2008, 59: 663–668

[62] Pardo A, Merino M, Coy A, et al. Influence of Ti, C and N concentration on the intergranular corrosion behaviour of AISI 316Ti and 321 stainless steels. Acta Materialia, 2007, 55: 2239–2251

[63] https://www.met-tech.com/316ti-stainless-steel-preheater-tube/ (Accessed July 2020)

[64] https://www.nace.org/resources/general-resources/corrosion-basics/group-3/stress-corrosion-cracking (Accessed July 2020)

[65] Tuck CDS, Powell CA, Nuttall J. Corrosion of Copper and Its Alloys. Shreir's Corrosion, 2010; 3: 1937-1973

[66] Papavinasam S. Corrosion Control in the Oil and Gas Industry. Gulf Professional Publishing, 2013

[67] https://www.indiamart.com/proddetail/dezincification-testing-service-iso-6509-21631919791.html (Accessed July 2020)

[68] http://www.andersonmaterials.com/graphitic-corrosion-cast-iron.html (Accessed July 2020)

[69] Zeng L, Zhang G, Guo X. Erosion–corrosion at different locations of X65 carbon steel elbow. Corrosion Science, 2014, 85: 318–330

[70] Jones M, Llewellyn. Erosion–corrosion assessment of materials for use in the resources industry. Wear, 2009, 267: 2003–2009

[71] http://www.cdcorrosion.com/mode_corrosion/corrosion_image/erosion_zoom.jpg (Accessed July 2020)

[72] High temperature corrosion and materials applications. ASM International, 2007

[73] Nissen DA. The chemistry of the binary $NaNO_3$-KNO_3 system. SAND81-8007. Sandia National Laboratories, 1981
[74] Baraka A, Abdel-Rohman AI, EI Hosary AA. Corrosion on mild steel in molten sodium nitrate-potassium nitrate eutectic, British Corrosion Journal, 1976; 11: 44–46.

[75] De Jong, J, Broers G. Electrochemistry of the oxygen electrode in the KNO3î—¸KO2 system, a comparative study. Electrochimica Acta, 1977; 22: 565-571

[76] Sultan S, Balakrishnan K. Cyclic voltammetric behaviour of platinum in dried and wet nitrates melt. Electrochimica Acta, 1993; 38: 2611-2615

[77] El Hosary A, Shams El Din A. A chronopotentiometric study of the stability of oxide ion in molten nitrates. Electrochimica Acta, 1971; 16: 143-149

[78] https://www.sqm.com/en/producto/sales-termo-solares/ (Accessed July 2020)

[79] H.J. Grabke, E. Reese, M. Spiegel, The effects of chlorides, hydrogen chloride, and sulfur dioxide in the oxidation of steels below deposits, Corrosion Science, 1995; 37: 1023-1043

[80] Prieto C, Ruiz-Cabañas FJ, Rodríguez-Sánchez A, Rubio C, Fernández AI, Martínez M, Oró E, Cabeza LF. Effect of the impurity magnesium nitrate in the thermal decomposition of the solar salt. Solar Energy, 2019; 192: 186-192

[81] Arroyave C, Morcillo M. The effect of nitrogen oxides in atmospheric corrosion of metals. Corrosion Science, 37; 1995: 293-305

[82] Osarolube, E, Owate IO, Oforka NC. Corrosion behavior of mild and high carbon steels in various acidic media. Scientific Research and Essay, 2008; 3: 224-228

[83] Smith GP. Corrosion of materials in fussed hydroxides. ORNL-2048. Oak Ridge National laboratories, 1956

[84] L. Cabeza, E. Galindo, C. Prieto, C. Barreneche, A. Fernández, Key performance indicators in thermal energy storage: Survey and assessment, Renewable Energy, 83; 2015: 820–827

[85] M. Liu, N.H. Steven, S. Bell, M. Belusko, R Jacob, G. Will, W. Saman, F. Bruno, Review on concentrating solar power plants and new developments in high temperature thermal energy storage technologies, Renewable and Sustainable Energy Reviews, 53; 2016: 1411–1432

[86] L. Sena-Henderson, Advantages of using molten salts, SANDIA National Laboratories, 2006

[87] Goods H. Bradshaw HR, Prairie M, Chavez J. Corrosion of stainless steels and carbon steels in molten mixtures of industrial nitrates (SAND 94-8211), SANDIA National laboratories, 1994

[88] Kruizenga A, Gill D, LaFord M, McConohy G. Corrosion of High Temperature Alloys in Solar Salt at 400, 500, and 680°C (SAND 2013-8256), SANDIA National Laboratories, 2013

[89] Bradshaw R, Oxidation and Chromium Depletion of Alloy 800 and 316SS and by Molten NaNO3 - KNO3 at Temperatures above 600°C (SAND86-9009), SANDIA National Laboratories, 1987

[90] Bradshaw R, Goods S. Corrosion Resistance of Stainless Steels during Thermal Cycling in Alkali Nitrate Molten Salts (SAND2001-8518), SANDIA National Laboratories, 2001

[91] Bradshaw R. Accelerated Corrosion Testing of a Nickel-Base Alloying a Molten Salt (SAND2001-8758), SANDIA National Laboratories, 2002

[92] Prieto C, Osuna R, Fernandez AI, Cabeza L, Molten salt facilities, lessons learnt at pilot plant scale to guarantee commercial plants; heat losses evaluation and correction, Renewable Energy, 2016; 94: 175-185

[93] ASTM G4-01: Standard guide for conducting corrosion tests in field applications, ASTM International

[94] ASTM G30-95. Standard Practice for Making and Using U-Bend Stress-Corrosion Test Specimens, ASTM International

[95] ASTM G58-85. Standard Practice for Preparation of Stress-Corrosion Test Specimens for Weldments, ASTM International

[96] ASTM G78-01. Standard Guide for Crevice Corrosion Testing of Iron-Base and Nickel-Base Stainless Alloys in Seawater and Other Chloride-Containing Aqueous Environments, ASTM International

[97] R.W. Bradshaw, W. M. Clift, Effect of chloride content of molten nitrate salt on corrosion of A516 carbon steel (SAND 2010-7594), SANDIA National laboratories, 2010

[98] CES Selector 2016 Software, Granta Design Ltd, Cambridge, 2016

[99] Ashby MF, Shercliff H, Cebon D. Materials: Engineering, Science, Processing and Design, 2nd ed., Butterworth Heinemann, Oxford, 2010, 203–224

[100] https://solarpaces.nrel.gov/by-technology/parabolic-trough (Accessed July 2020)

[101] Chen J, Xiao J, Zhang Y, Wei Y, Han B, Li Y, Zhang S, Li N. Corrosion mechanism of Cr2O3-Al2O3-ZrO2 refractories in a coal-water slurry gasifier: A post-mortem analysis. Corrosion Science, 2020; 163: 108250

[102] Alvarenga RA, Lenz GF. A statistical and post-mortem study of wear and performance of MgO-C resin bonded refractories used on the slag line ladle of a basic oxygen steelmaking plant. Engineering Failure Analysis, 2017; 78: 161-168

[103] Belgacem S, Galai H, Tiss H. Qualitative and quantitative investigation of post–mortem cement refractory: The case of magnesia–spinel bricks. Ceramics International, 2016; 42: 19147-19155

[104] Nag M, Agrawal T, Singh B, Biswas S. Study and post mortem analysis of steel ladle porous plug to improve bottom purging efficiency for cleaner steel. Engineering Failure Analysis, 2019; 101: 447-455

[105] German PA, Hill AC, Taylor MR. Mild steel oxidation in CO2-cooled reactors. Gas Cooled Reactors Today. Proceedings of the conference, Bristol, 20-24, 1982

[106] Yogev R, Kribus A. Operation strategies and performance of solar thermal power plants operating from PCM storage. Solar Energy, 2013; 95: 170-180

[107] Xu B, Li P, Chan C. Application of phase change materials for thermal energy storage in concentrated solar thermal power plants: A review to recent developments. Applied Energy, 2015; 160: 286-307

[108] Feldhoff JF, Schmitz K, Eck M, Schnatbaum-Laumann L, Laing D, Ortiz-Vives F, Schulte-Fischedick J. Comparative System Analysis of Parabolic Trough Power Plants with DSG and Oil using Integrated Thermal Energy Storage, Solar Energy, 2012; 86: 520–530

[109] Jové A, Prieto C, Abujas C, Rodríguez-Sánchez A, Alguacil M. Heat storage method and system for a solar steam generation plant and solar steam generation plant. WO 2016/034754

[110] Jové A, Prieto C. Heat storage system and method for the charging and discharging thereof. WO 2014053677 A1

[111] Abe Y, Kamimoto M, Kanari K, Ozawa T, Sakamoto R, Takahashi Y. Peak load coverage by molten salts latent thermal storage. Proceedings of 19th intersociety energy conversion engineering conference; 1984; 2: 1114–1119

[112] Palomo E, Khemis S, Mourand D, Noel F, Ho-Kon-Tiat V, Dauverge JL, Anguy Y, Prieto C, Jové A. Composite material for storing heat energy at high temperatures. EP 2444468 A1

[113] Bozzini B, Barella S, Bogani, F, Giovannelli G, Natali S, Scarselli G, Boniardi M. Corrosion of stainless steel grades in molten NaOH/KOH eutectic at 250 °C: AISI304 austenitic and 2205 duplex. Materials and Corrosion, 2012; 63: 967-978

[114] Craighead CM, Smith LA, Jaffee RI. Screening Tests on Metals and Alloys in Contact with Sodium Hydroxide at 1000 and 1500 °F, OAK Ridge National Laboratory - U.S. Atomic Energy Commission, Report BMI-705, 1951

[115] Simmons EM, Miller NE, Stang JH, Weaver C. Corrosion and Components Studies on Systems Containing Fused NaOH, U.S. Atomic Energy Commission, Report BMI-1118, 1956

[116] Lad RA, Simon SL. A Study of Corrosion and Mass Transfer of Nickel by Molten Sodium Hydroxide, Corrosion, 1954; 10 (12): 435-439

[117] Gregory JN, Hodge N, Iredale JVG. The Static Corrosion of Nickel and Other Materials in Molten Caustic Soda, Atomic Energy Research Establishment, Harwell, U.K., 1956

[118] Design guidelines for the selection and use of stainless steel. Nickel development institute

[119] Klueh RL. Chromium-Molybdenum steels for fusion-reactor applications. Oak Ridge National Laboratory

[120] Klueh RL, Nelson AT. Ferritic/martensitic steels for next generation reactors. Journal of Nuclear Materials, 2007; 371: 37-52

[121] Viswanathan R, Puerget R, Rao U. Materials technology for advanced coal power plants

[122] Farrar JCM. The Alloy Tree. A Guide to Low-Alloy Steels, Stainless Steels and Nickel-base Alloys. Woodhead publishing limited, 2004

[123] Ivanov SO, Gorbatykh VP. The Effects of a Lithium–Ferritic Film on Slowing Down Corrosion Cracking of Heat-Exchange Tubes of Steam Generator at Nuclear Power Plants with VVER Reactors. Thermal Engineering, 2007; 54: 332–335

[124] Lim T, Hwang ER, Ha HY, Nam SW, Hong SA. Effects of temperature and partial pressure of CO2/CO on corrosion behavior of stainless-steel in molten Li/Na carbonate salt. Journal of Power Sources, 2000; 89: 1-6